DEVELOPMENT, SETUP AND TESTING OF A DYNAMIC HYDRAULIC FRACTURE CONDUCTIVITY APPARATUS

A Thesis

by

POTCHARAPORN PONGTHUNYA

Submitted to the Office of Graduate Studies of
Texas A&M University
in partial fulfillment of the requirements for the degree of

MASTER OF SCIENCE

August 2007

Major Subject: Petroleum Engineering

DEVELOPMENT, SETUP AND TESTING OF A DYNAMIC HYDRAULIC FRACTURE CONDUCTIVITY APPARATUS

A Thesis

by

POTCHARAPORN PONGTHUNYA

Submitted to the Office of Graduate Studies of
Texas A&M University
in partial fulfillment of the requirements for the degree of

MASTER OF SCIENCE

Approved by:

Chair of Committee,	A. Daniel Hill
Committee Members,	Stephen A. Holditch
	Michael Sherman
Head of Department,	Stephen A. Holditch

August 2007

Major Subject: Petroleum Engineering

ABSTRACT

Development, Setup and Testing of a Dynamic

Hydraulic Fracture Conductivity Apparatus. (August 2007)

Potcharaporn Pongthunya, B.Eng., Chulalongkorn University

Chair of Advisory Committee: Dr. A. Daniel Hill

One of the most critical parameters in the success of a hydraulic fracturing treatment is to have sufficiently high fracture conductivity. Unbroken polymers can cause permeability impairment in the proppant pack and/or in the matrix along the fracture face. The objectives of this research project were to design and set up an experimental apparatus for dynamic fracture conductivity testing and to create a fracture conductivity test workflow standard. This entirely new dynamic fracture conductivity measurement will be used to perform extensive experiments to study fracturing fluid cleanup characteristics and investigate damage resulting from unbroken polymer gel in the proppant pack.

The dynamic fracture conductivity experiment comprises two parts: pumping fracturing fluid into the cell and measuring proppant pack conductivity. I carefully designed the hydraulic fracturing laboratory to provide appropriate scaling of the field conditions experimentally. The specifications for each apparatus were carefully considered with flexibility for further studies and the capability of each apparatus was defined.

I generated comprehensive experimental procedures for each experiment stage. By following the procedure, the experiment can run smoothly. Most of dry runs and experiments performed with sandstone were successful.

DEDICATION

To my parents, uncle, aunt and brothers, for their infinite support and encouragement throughout my study.

ACKNOWLEDGMENTS

I would like to express my sincere gratitude to my advisors: Dr. A. Daniel Hill and Dr. Ding Zhu for offering me the opportunity to work on this project and for guiding me throughout the work. Thanks for your encouragement and your patience.

Thanks to the hydraulic fracturing team: Feiyan Chen, Fivman Marpaung, Xiaoze Jin, and Pavalin Limthongchai for your help and suggestion throughout the experimental setup. Special thanks to Feiyan Chen and Fivman Marpaung who were always with me during preliminary testing.

Thanks also to Dr. Stephen A. Holditch and Dr. Michael Sherman for serving as committee members and to Maysam Pournik, Maria Gina Melendez and Frank Platt for their help and support in my graduate study. I also want to extend my gratitude to the Crisman Institute at the Department of Petroleum Engineering at Texas A&M University for funding the research project.

TABLE OF CONTENTS

Page

Page

LIST OF FIGURES

FIGURE Page

LIST OF TABLES

CHAPTER I

INTRODUCTION

1.1 Hydraulic fracturing in tight gas reservoirs

Tight gas reservoirs are an unconventional resource found at all depths. In general, these types of reservoirs cannot be economically developed without the use of hydraulic fracturing.

Hydraulic fracturing is a main technique of well stimulation in low-permeability reservoirs. The first fracturing treatment was introduced to the industry in 1947 in the Hugoton gas field in an effort to increase well deliverability of four acidized limestone pay zones. By 1988, over a million fracturing treatments had been performed.[1] Hydraulic fracturing has played a major role in enhancing petroleum recovery reserves and daily production. The concept of hydraulic fracturing is to change the reservoir flow pattern by creating a long and highly conductive flow path in the reservoir. With the fracture, reservoir fluids flow briefly through the low permeability reservoir into the fracture; then, the fluids easily flow through the high permeability proppant pack into the wellbore. In addition, the flow also bypasses the near-wellbore damage zone.

This thesis follows the style of *Journal of Petroleum Technology*.

To initiate the fracture and establish propagation in a target reservoir, viscous fracturing fluid called a pad is injected at high pressure, higher than the formation breakdown pressure. Then, a slurry of viscous fluid mixed with propping agent or proppant is pumped into the fracture to extend the fracture and concurrently carry the proppant deep into the fracture. In this process, sufficient quantities of proppant are required to prevent the fracture from closing after the fluid injection is stopped and to create a highly conductive proppant pack. After finished pumping, the viscous fluid must break back to a low viscosity so that the fracturing fluid can clean up and leave only the highly conductive proppant pack in the fracture. A typical hydraulic fracturing treatment consists of pumping pre-pad, pad, slurry, and flush, respectively.

Although many different types of fracturing fluids such as water-based polymer solutions, polymer water-in-oil emulsions, and aqueous foams are currently available, the majority of fracturing fluid used is the water-based polymer, because it performs well in a wide range of formation types, depths, pressure, and temperature at relatively low cost. In addition to the base fluid, many additives including fluid-loss additives, breakers, and buffers are added to perform different functions. In deep reservoirs, high concentrations of high-strength proppant are pumped to keep the fractures open. The high viscosity of the slurry is needed to carry a large amount of proppant deep into the fractures. Obtaining higher viscosity in linear gels means increasing polymer concentration. In the 1960s, when crosslinked fracturing fluid was first used, it was considered a major advancement in hydraulic fracturing technology.[2] Nowadays, the crosslinked fluids are generally used in fracturing treatments because of their better proppant carrying and higher temperature stability.

One of the most critical parameters in the success of a hydraulic fracturing treatment is to have sufficiently high fracture conductivity. In general, higher fracture conductivity yields better well productivity. Factors affecting fracture conductivity include formation closure stress, proppant particle size and size distribution, proppant concentration, proppant strength, proppant grain shape, and fracturing fluid residue. The

residue, or gel damage, is a product of the degradation of the polymer used to create viscosity in the fracturing fluid. Unbroken polymers can cause permeability impairment in the proppant pack and/or in the matrix along the fracture face. The main flow in a fractured well comes from the fracture itself which has very large surface area. Damage to the permeability of the proppant pack is much more likely to cause significant impairment to well productivity than damage to the matrix permeability around the fracture.

1.2 Review of literature

Fracturing fluid cleanup characteristics and gel damage can be determined only by conducting laboratory experiments. The investigation analyzes fracture conductivity changing with flowback time by varying proppant concentration, polymer concentration, injection rate and duration, temperature, and gas flow rate. Typically, the proppant pack conductivity testing follows API RP 61.[3] The recommended procedure is to load a known amount of proppant (generally 2 lb/ft^2) uniformly between two metal platens, put them into the conductivity cell, apply a hydraulic pressure, flow test fluid through the cell, measure differential pressure and flow rate, and calculate the conductivity.

Cooke[4] studied the reduction of proppant pack conductivity caused by fracturing fluid residue. In his experiments, fracturing fluid mixtures consisted of various polymers in a concentration range from 50 to 480 lb/1,000 gal, various breakers, and fluid loss additives, but no crosslinker. The reduction of pore space of the proppant pack was measured and related to a predicted reduction in permeability and conductivity. Permeability and conductivity were measured at difference stresses by flowing fracturing fluid without proppant into the heated cell that had proppant pack with a width of 0.6 in. sandwiched between two rocks. The measured results were then compared to the predictions. The results showed that the guar polymer residue was the most important material that affected fracture conductivity reduction. This early work did not properly simulate the actual fracturing applications because of too high polymer

concentration with no crosslinker, and too wide fracture width. Last but not least, the proppant was placed into the cell artificially.

Almond and Bland[5] investigated the effect of the break mechanism on gel residue and flow impairment of 20/40 mesh sand caused by gel damage. The residue content (percent by weight) and the relative residue volume produced from different guar gum polymers were determined. However, they conducted their experiments on a sand-pack cell without a rock sample and applied no stress on the proppant.

Roodhart, Kulper, and Davies[6] investigated the proppant pack conductivity by taking into account the fluid cleanup period. They used nitrogen gas in the flowback period to simulate gas well conditions. Their design was to put a clean core sample on top of the proppant bed in a cell and measure conductivity at the desired condition; then they injected gel from the bottom line through the proppant pack to generate a filter cake. The nitrogen gas was flowed from the top line through the core and proppant bed to simulate the cleanup period. After that, the conductivity was again measured. Although the study tried to simulate a fractured gas well, the experiments were conducted on only one core face with the artificial proppant pack.

In 1987, Penny[7] conducted experiments by flowing slurry into the conductivity cell to study fracturing fluid interactions. However, they did not investigate the fracturing fluid clean up characteristics. Parker and McDaniel[8] presented an effect of fluid loss filter cakes on the fracture conductivity. Their results showed that gel damaged decreased the fracture conductivity under the same closure stress over time. However, their experiments did not consider fluid cleanup. They merely left the cell at the desired closure stress for a desired time without flowing fluid.

Hawkins[9] studied the clean up characteristics and gel damage. He concluded that maximizing proppant pack permeability when using water-based fracturing fluid requires minimizing the use of crosslinker, polymer concentration and shut in time, and maximize sand concentration, proppant size and breaker content. His experiments,

however, were conducted by placing a desired amount of proppant into the cell and flowing deionized water through the cell to simulate the cleanup period.

McDaniel[10] conducted experiments by injecting slurry into the conductivity cell, flowing KCl brine water to measure conductivity for one or more days, and changing to wet nitrogen later. His study focused on fracture conductivity measurement, not fluid cleanup characteristics.

This research, therefore, develops a new laboratory apparatus and provides a new recommended testing procedure to study fracturing fluid cleanup characteristics and investigate damage resulting from unbroken polymer gel in the proppant pack.

1.3 Research objectives

The objectives of this research project are to design and set up an experimental apparatus for dynamic fracture conductivity testing and create a fracture conductivity test workflow standard. This entirely new dynamic fracture conductivity measurement will be used to carry out extensive experiments to study fracturing fluid cleanup characteristics and investigate damage resulting from unbroken polymer gel in the proppant pack.

Unlike conventional fracture conductivity tests in which a known amount of proppant is loaded into the fracture conductivity cell artificially, we design to pump a slurry into a fracture conductivity cell dynamically. This dynamic fracture conductivity test simulates the proppant placement conditions that actually occur during hydraulic fracturing treatments. In the experiments, fracturing fluid with proppant is pumped into a fracture conductivity cell at injection rates representative of conditions in an actual fracturing job. After fracturing fluid is flowed for some length of time, the cell is shut in for some period with closure stress applied to simulate shut in duration in the field; then nitrogen gas flows through the cell to represent the flowback period. Finally, the

conductivity of the fracture with the proppant trapped in the fracture after the simulated treatment is measured.

For further investigation of gel damage, the experimental parameters including proppant concentration, polymer concentration, injection rate and duration, temperature, and gas flow rate will be studied carefully. Therefore, the specifications for each part of the apparatus are carefully considered. The goals are to assemble the equipment in a timely and cost-effective manner and to develop an easily operable laboratory with flexibility for further studies.

The dynamic fracture conductivity experiment can divide into two parts: pumping fracturing fluid into the cell and measuring proppant pack conductivity. In the pumping part, the main components of the apparatus are a mixing tank to prepare base gel and slurry mixture, a base gel tank, a series of multistage centrifugal pumps to inject fluid at high pressure, cylindrical heaters and heating jacket to build fluid temperature up to reservoir conditions, a modified API fracture conductivity cell, a load frame to apply closure stress, a flow system with leakoff capability, a high-pressure vessel with a needle valve to control flow rate, and auxiliary equipment. The equipment for conductivity measurement consists of a nitrogen tank to supply gas, a mass flow controller to control and measure gas flow rate, a water chamber to simulate wet gas, a heated conductivity cell under stress of the load frame, and a backpressure regulator to control pressure. All experimental variables are measured and recorded; then, the experimental result is interpreted.

The steps for each dynamic fracture conductivity experiment are as follows:

- Core sample preparation and assembly
- Rock permeability measurement
- Fracturing fluid preparation and injection through the conductivity cell
- Proppant pack conductivity measurement

We generated comprehensive experimental procedures for each experiment stage. The laboratory setup includes specifications of each experimental apparatus. Results of several preliminary tests lead to recommendations for future experimental studies and lessons learned.

CHAPTER II

DESIGN AND SETUP OF HYDRAULIC FRACTURE CONDUCTIVITY LABORATORY

The dynamic fracture conductivity experiment comprises two parts: pumping fracturing fluid into the cell and measuring proppant pack conductivity. The pumping part is a new design, whereas the conductivity measurement is modified from the existing acid fracture laboratory.[11]

2.1 Design of experiments

The project objectives are to design and set up an experimental apparatus for dynamic fracture conductivity testing. The new laboratory was developed with goals to simulate the proppant placement conditions that actually occur during hydraulic fracturing treatments in fields and to use appropriate scaling to represent the field condition experimentally with flexibility for further studies of gel damage and fluid cleanup characteristics. The specifications for each apparatus therefore were carefully considered.

In typical field treatment designs, the flow rate ranges from 15 bbl/min to 50 bbl/min and the slurry concentration ranges from 1 ppg to 8 ppg. The estimated fracture width during pumping is from 0.2 to 0.5 in. and the estimated fracture height typically ranges from 50 ft to 200 ft. In this experimental setup, a flow rate of 25 bbl/min, a slurry concentration of 2 ppg, a leakoff differential pressure of 1,000 psi, a fracture width of 0.25 in., and a fracture height of 100 ft were selected to calculate the laboratory conditions. Table 2.1 provides the typical field treatment design used to determine the laboratory conditions.

Table 2.1- Typical field treatment design used to design laboratory conditions

Pumping rate *(q)*	25 bbl/min	0.066 m^3/sec
Fracture height *(h)*	100 ft	30.48 m
Fracture width *(wf)*	0.25 inch	0.0064 m
Fluid density *(ρ)*	1,000 kg/ m^3	
Proppant concentration	2 ppg	
Leakoff Δp	1,000 psi	

To mimic actual field conditions in the laboratory, we matched the flux of fracturing fluid along the fracture. The flux is a rate of flow across area (*q/A*). If the flux of fracturing fluid along the fracture in the laboratory is close to the field treatments, the pumping condition in the laboratory is comparable to that of field fracturing jobs.

In the fracturing treatments, the fracturing fluid is injected into two wings of fracture. Therefore,

$$q_{field} = 2(v_{field} w_{f,field} h_{field}) \quad \text{..... (2.1)}$$

Thus, the flux along the fracture is:

$$v_{field} = \frac{q_{field}}{2 w_{f,field} h_{field}} \quad \text{..... (2.2)}$$

From Eq. 2.2,

$$v_{field} = \frac{0.066\ m^3/\text{sec}}{2(0.0064\ m)(30.48\ m)} = 0.1692\ m/\text{sec} = 33.307\ ft/\text{min}$$

In the experiments, the fracturing fluid is pumped into one fracture in the conductivity cell. Hence,

$$q_{lab} = v_{lab} w_{f,lab} h_{lab} \quad \text{..... (2.3)}$$

To simulate the field condition in the experiment, $v_{field} = v_{lab}$. The width of the core samples, which corresponds to the fracture height, is 1.75 in. or 0.044 m. By assuming the small fracture width of 0.25 in. or 0.0064 m, the designed pumping rate in the experiments is

$$q_{lab} = v_{field} w_{f,lab} h_{lab} \quad \text{..... (2.4)}$$

$$q_{lab} = (0.1692\ m/\sec\ )(0.0064\ m)(0.044\ m)$$

$$q_{lab} = 4.76\times10^{-5} m^3/\sec\ \ or\ 2.86\ L/\min\ \ or\ 0.76\ gal/\min$$

From the fluid flux calculation, a flow rate of at least 0.76 gal/min is required to simulate the actual field treatments in the laboratory scale.

2.2 Leakoff pressure profiles after shut-in

In low permeability reservoirs, the fluid loss into the fracture is a transient flow process. The solution of the differential equation for the leakoff pressure is modified from the solution of the differential equation of temperature in the semi-infinite solid (Eq.2.5).[12]

$$\frac{\partial v}{\partial t} = \kappa \frac{\partial^2 v}{\partial x^2}, \quad \text{..... (2.5)}$$
$$v = 0 \ \ for\ t = 0 \ \ and\ v = \phi(t) \ \ at\ x = 0$$

In the case of $\phi(t) = V_0$, constant, $0 < t < T$, the solution is:

$$v = V_0 erfc \frac{x}{2\sqrt{(\kappa t)}},\ 0 < t < T \quad \text{..... (2.6)}$$

The differential equation for the leakoff pressure is:

$$\frac{\partial^2 p}{\partial x^2} = \frac{\mu c_t \phi}{k} \frac{\partial p}{\partial t}, \quad \text{..... (2.7)}$$

From Eqs. 2.5 and 2.6, let $\nu = p$ and $\kappa = \frac{k}{\phi \mu c_t}$, the solution of the differential equation for the leakoff pressure is:

$$p = p_{frac} erfc \frac{x}{2\sqrt{\frac{kt}{\phi \mu c_t}}} \quad \text{..... (2.8)}$$

Fig. 2.1 shows leakoff pressure profiles of the reservoir with the permeability of 0.1 md, the fluid viscosity of 1 cp, the total compressibility of 0.00001 psi^{-1} and the porosity of 0.1. We assumed a reference reservoir pressure of 0 psi; at $t = 0$, the fracture pressure becomes 2,000 psi. Fig. 2.1 shows how the pressure very near the fracture face changes with time. We used this result to guide our selection of the fluid loss differential pressure. The 300 psi fluid loss differential pressure in our experiments (Section 2.3.1) represents the differential pressure expected after a few minutes of fracture time.

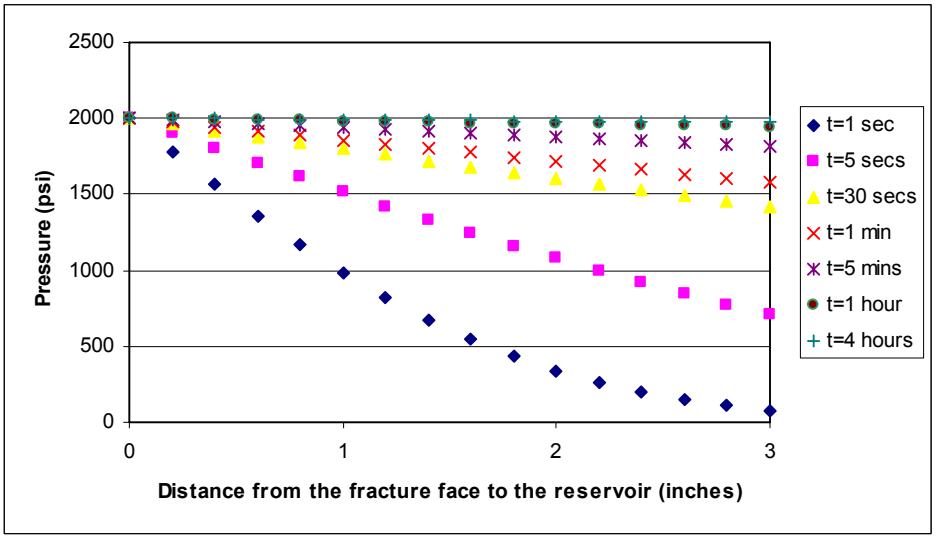

Fig. 2.1- Pressure profiles from the fracture face to the reservoir of 0.1 md rock permeability.

2.3 Setup of fracturing fluid pumping experiments

The pumping apparatus consists of a mixing tank to prepare the base gel and slurry mixture, a base gel tank, a series of multistage centrifugal pumps to pump fluid at high-pressure conditions, cylindrical heaters and heating jacket to build fluid temperature up to reservoir conditions, a modified API fracture conductivity cell, a load frame to apply closure stress, a flow system with leakoff capability, a high-pressure vessel with a needle valve to control flow rate, and auxiliary equipment as shown in Fig. 2.2. Flow lines before the high-pressure pumps are 3/4-in. PVC. All flow lines after the high-pressure pump except the leakoff lines are 1/2-in. stainless steel because of high-pressure and high temperature fluid. The leakoff lines are 1/8-in. stainless steel. Various ball valves and bypass lines are designed for pump cleaning after finishing each experiment.

The polymer solutions for both base gel and slurry are prepared in the mixing system. The base gel is then transferred to the base gel tank by a small centrifugal pump. After that, proppant and other chemicals are added into the mixer to prepare a slurry. The base gel is fed into multistage centrifugal pumps by a small centrifugal pump, flows through cylindrical heaters, and enters the conductivity cell. The fluid flows into a high-pressure vessel and goes into a waste tank. The pressure is controlled by needle valves installed at the outlet of the high-pressure vessel. After base gel is injected, slurry is pumped into the multistage centrifugal pumps while crosslinker is added into the system by a metering pump on the fly. The cell pressure and leakoff pressure are recorded by pressure transmitters. The flow rate is measured downstream of the high-pressure vessel. The conductivity cell is then left shut in for some length of time under the desired temperature to simulate the shut-in period. The fracture is closed by applying a fixed closure stress to the cell during the shut-in period. After that, the fracture conductivity measurement is performed.

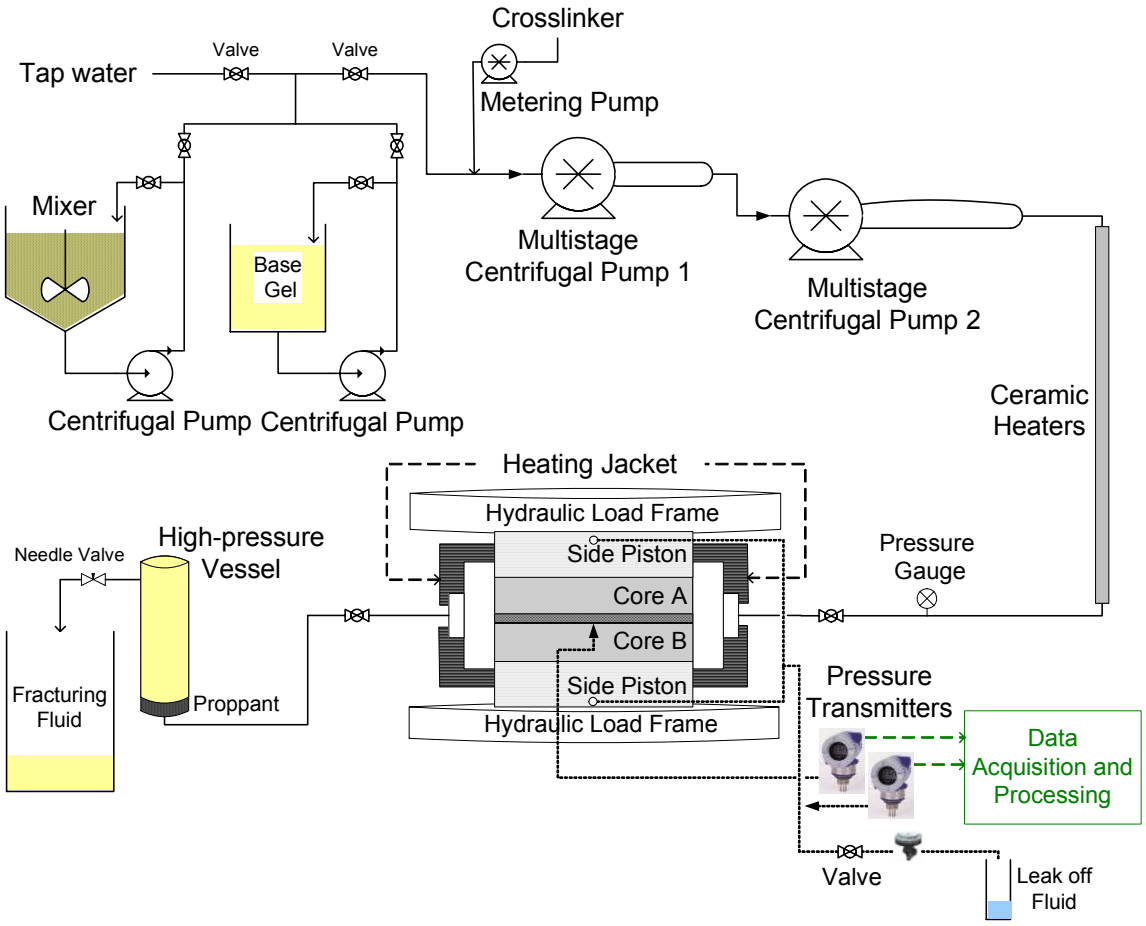

Fig. 2.2- Schematic of dynamic fracture conductivity laboratory setup for pumping.

2.3.1 Core samples

Rock samples used in the hydraulic fracture conductivity experiments are low-permeability sandstone. The rocks are custom cut to a rectangular shape with rounded edges to fit into the conductivity cell with approximately 0.07 in. space in all dimensions. The core dimensions are 7 in. long, 1.65 in. wide, and 3 in. in height. Each core sample is then put in a mold and potted with silicone potting compound. The silicone rubber around the rocks provides a seal between the core and the conductivity cell. However, after several experiments, we found that the rubber could not fully prevent fluid from flowing in the gap between the rubber and the cell's wall. Therefore,

the core samples are wrapped with Teflon tape to prevent leaks. After several tests, we concluded that the Teflon tape can prevent leakage if the differential pressure is less than 300 psi. The dimensions of the sample with silicone rubber are 7.25 in. long, 1.75 in. wide, and 3 in. in height. The round edges have a radius of 0.875 in. The surface area is about 12 in^2. Fig. 2.3 represents core sample preparation from a pure rock to molding with silicone rubber, then wrapping with Teflon tape. In the first phase of the experiments, we used dry cores. The core samples will be saturated with 2% KCl in the future experiments.

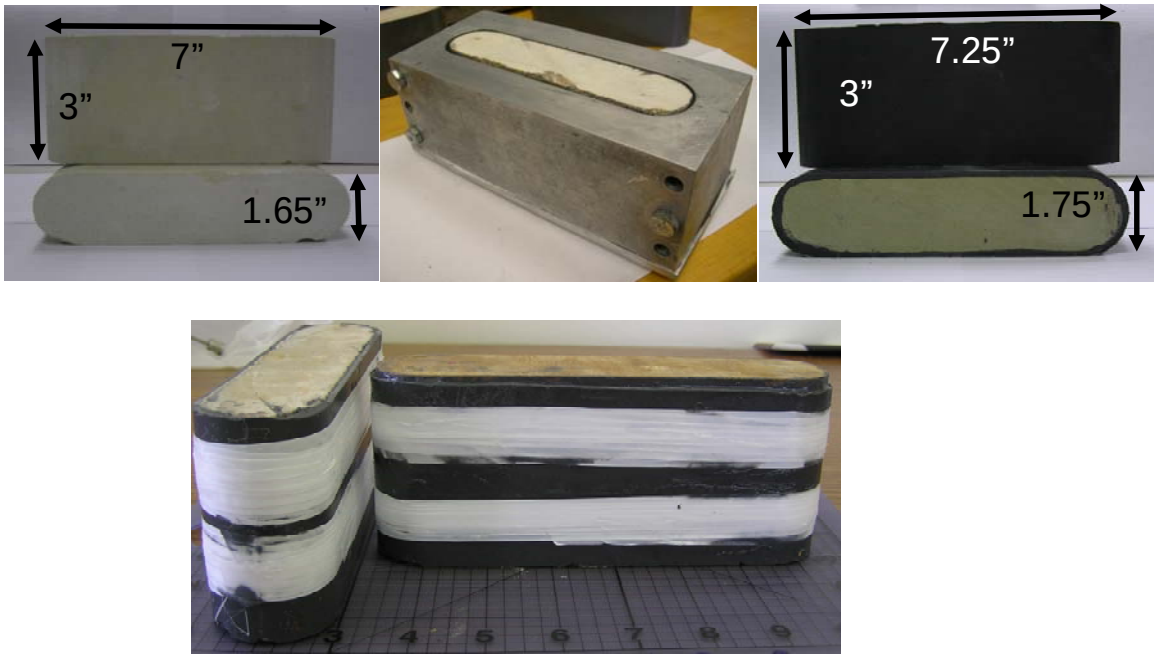

Fig. 2.3- Core sample preparation.

2.3.2 Modified API conductivity cell

The fracturing fluid is injected through a modified American Petroleum Institute (API) fracture conductive cell.[12] The cell consists of the cell body, two side pistons, and two flow inserts (Fig. 2.4). All parts are made of stainless steel with a rectangular shape

with rounded edges. Dimensions of the cell body are 10 in. long, 3-1/4 in. wide, and 8 in. in height. The cell body is designed to accommodate core samples 7 in. long, 1.65 in. wide, and 3 in. in height. One side of the cell body has three pressure access ports for pressure measurement. These ports are 7/16-in.-20 SAE/MS female threads that are connected to 4CMS4 Hoke fittings. The Swagelok inline filters model SS-4F-140, which have a 140 μm nominal pore size of strainer, are connected after the Hoke fitting to prevent proppant particles from plugging the 1/8-in. lines. The lines are connected to pressure transducers. Plugging in the line leads to an error in pressure reading. The side pistons with Viton polypack seal 25004500 VT90 are used to confine cores in the cell center and maintain a desired pressure inside the cell body during the experiments. The side piston cross-section area is 12.5 in^2. An access port in each piston is for matrix flowing: leakoff fluid while pumping and nitrogen during cleanup. The two flow inserts with Viton o-rings 2-123 VT90 at both ends of the cell body are attached to flow lines as an inlet and outlet. The total weight of the conductivity cell is approximately 110 lbs. The core samples are put inside the conductivity cell by a modified hydraulic jack[11].

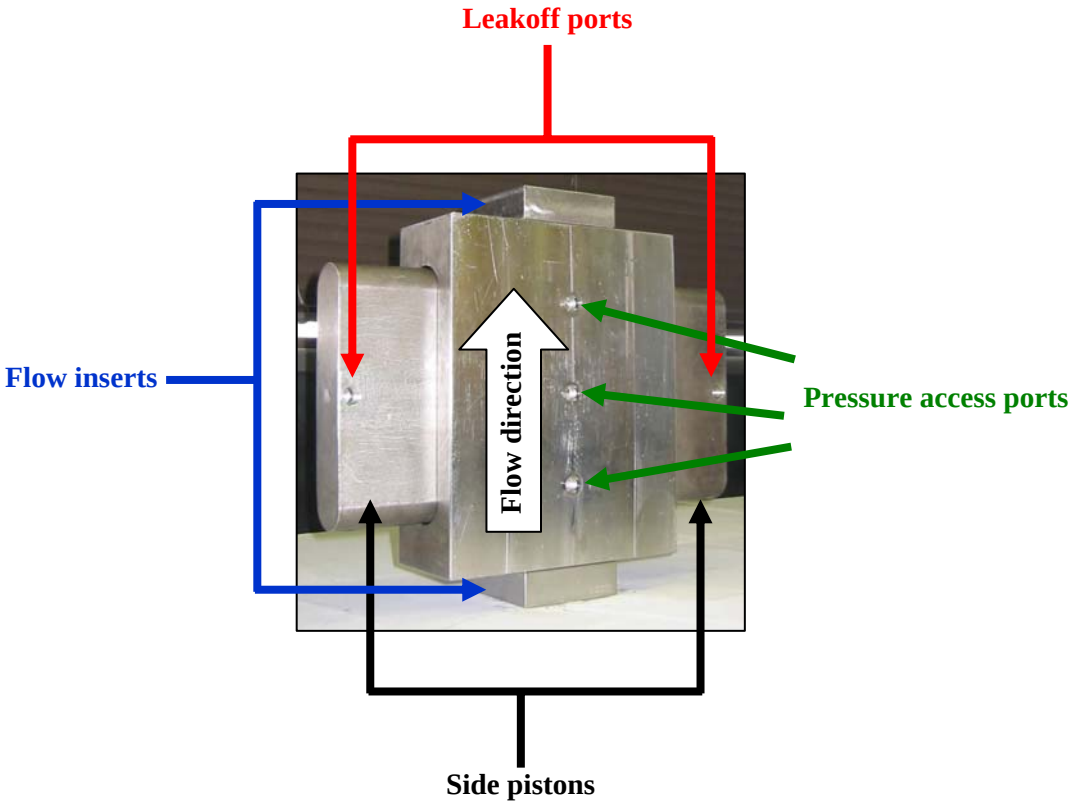

Fig. 2.4- Conductivity cell.

2.3.3 Chemicals and proppant

A service company supplied chemicals such as the Hydroxypropyl guar and the borate crosslinker with recipes used in actual fracturing jobs for the experiments. CARBO Ceramics provided 30/50 Econoprop for the experimental study. The particle diameters are from 0.0118 in. to 0.0236 in. with a median of 0.020 in. The reference permeability at 250°F under 2,000 psi closure stress is 230 Darcies. The specific volume is 0.044 gal/lb and the specific gravity is 2.70.

2.3.4 Mixing system

The mixing system consists of a 55-gallon alloy tank, a mixer, and a centrifugal

pump (Fig. 2.5). The mixer blends the mixture in the tank, and the centrifugal pump circulates the mixture from the bottom to the top. This design provides uniformly mixed slurry as revealed in Fig. 2.6. The mixing process starts with filling a desired volume of tap water for both base gel and slurry into the mixing tank via a flexible tube connected to the PVC tube. Polymer and pH buffer are added into the mixing tank to prepare the base gel while circulating with the mixer and the centrifugal pump. After mixing for 30 minutes, the base gel is then transferred to the 55-gallon polyethylene drum that is connected to another centrifugal pump used to drive the base gel into the high-pressure pump. Other additives and the desired amount of proppant are added into the mixing tank. Both pad and slurry are now ready to be pumped into the high-pressure pump.

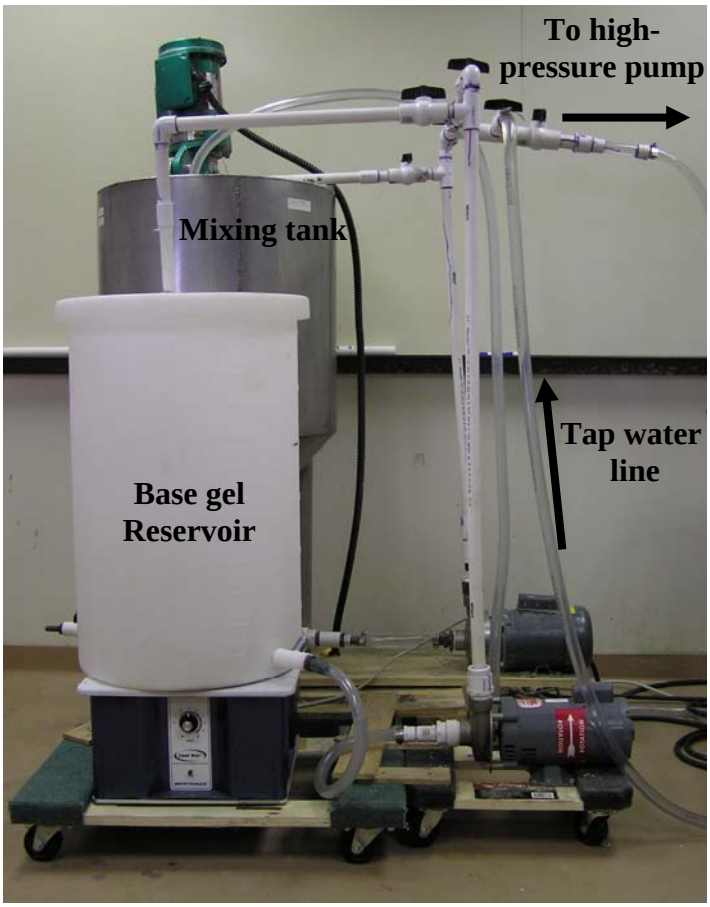

Fig. 2.5- Mixing system.

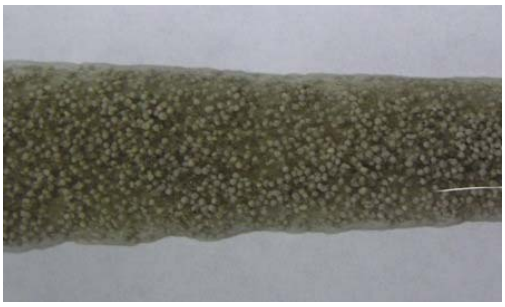

Fig. 2.6- Uniformly distributed slurry created by the mixing system.

2.3.5 Crosslinker pump

The crosslinker and crosslinker accelerator are mixed in a beaker and injected in the system while slurry flows into the high-pressure pump through a metering pump (Fig. 2.7). The crosslinker pumping rate is calculated from the pumping rate of the slurry and the mixture recipe provided by the service company and is adjusted based on the calibration chart in Fig. 2.8.

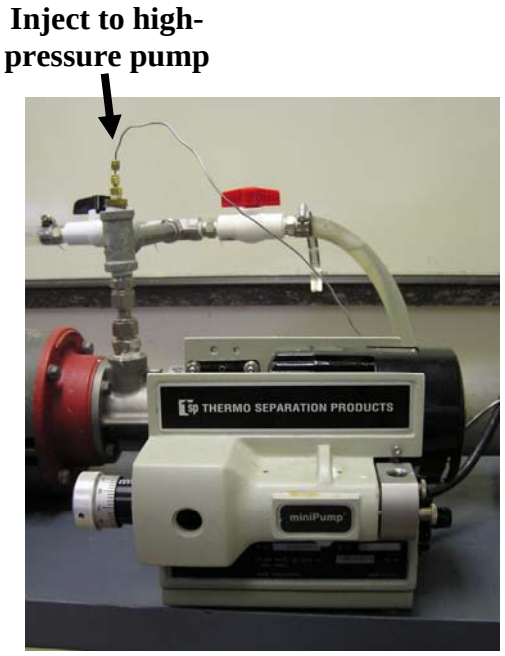

Fig. 2.7- Metering pump.

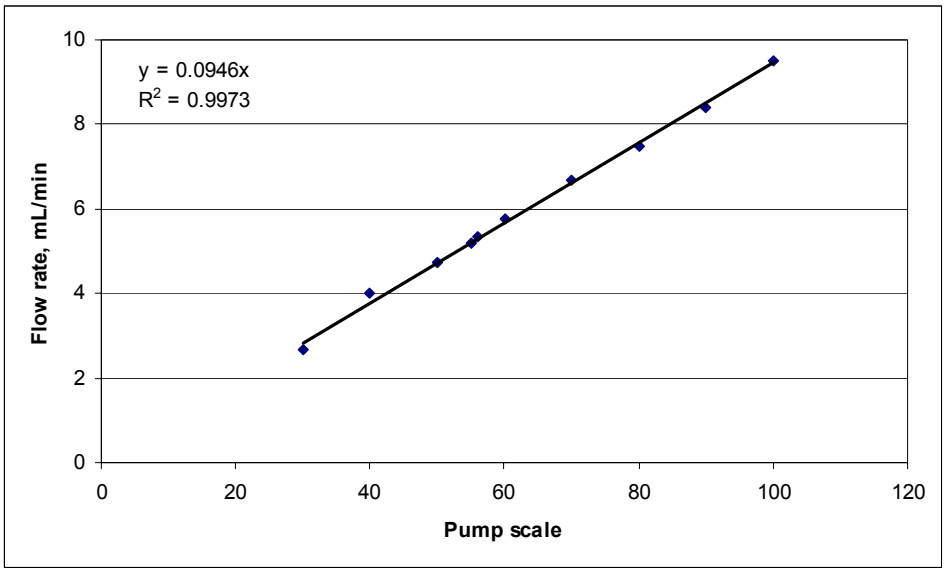

Fig. 2.8- Metering pump calibration at atmospheric pressure.

2.3.6 High-pressure pumps

To mimic field treatment conditions, the slurry is pumped at flow rates from 1 to 4 L/min at 1,000 psi. These flow rates reproduce the fluxes that occur in actual fracture treatments. Tonkaflo multistage centrifugal pumps, used to achieve the high pressure and flow rate, can pump the slurry from 1 to 5 gal/min at the designed pressures of 350 psi and 600 psi for the pump models SS538X and SS558G-50, respectively. To achieve the pressure of 950 psi, the pumps are aligned in series as shown in Fig. 2.9. The SS538X pump model, which has 38 stages, builds fluid pressure up to 350 psi before entering the 58-stages centrifugal pump SS558G-50 model, which increases the pressure to 950 psi. We changed the mechanical seals of the second pump to handle inlet pressures up to 400 psi. The maximum recommended operating temperature is 125°F. To extend the lifetime of the pumps, we flush them with water immediately after slurry injection to prevent the proppant from settling down inside the pumps. In the first phase of experimental studies, we used only the SS538X pump model.

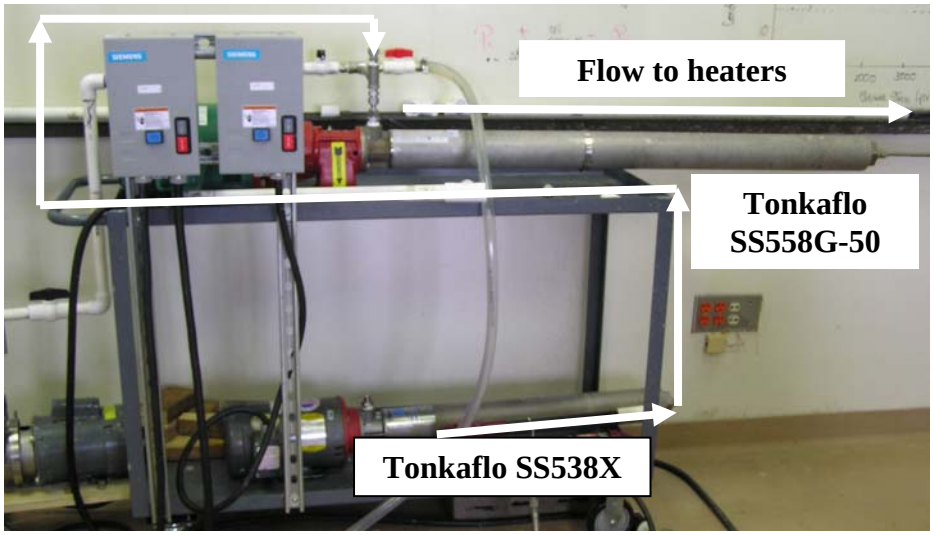

Fig. 2.9- Series of Tonkaflo multistage centrifugal pumps.

2.3.7 Cylindrical heaters and heating jacket

Temperature is a critical parameter in hydraulic fracturing treatments, and the breaking of fracturing fluid gels. To represent field conditions experimentally, the fracturing fluid is heated by cylindrical heaters before it enters the conductivity cell, which is wrapped with a heating jacket (Fig. 2.10). To study residual gel damage resulting from unbroken polymer, we conduct experiments at a temperature range of 150 to 250ºF. The fluid is heated to the desired temperature through six Omegalux CRWS series semi-cylindrical ceramic radiant heaters, 24-in. long and 1,200 watts. Two semi-cylindrical heaters are combined as a pair with the flow tubing in the center. The total length of the cylindrical heaters is 12 ft. A thermocouple installed downstream of the heaters is connected to a temperature controller. The controller is set to the desired temperature with 5ºF upper and lower ranges. The heaters are activated if the fluid temperature falls 5ºF below the desired temperature and deactivated if the temperature rises 5ºF above the desired temperature. A Glas-Col heating jacket heats the conductivity cell to simulate reservoir conditions. The 1/2-in. thick, 400 watts heating jacket is made from a fiberglass fabric heating mantle, custom cut to fit to the

conductivity cell and secured with straps. A thermal sensor pad attached between the heating jacket and the conductivity cell is connected to another temperature controller with the same setting as the temperature controller of the cylindrical heaters. The cylindrical heaters and their controller are turned off after the slurry is pumped, while the heating jacket remains on until the experiment is completed.

Fig. 2.10- Cylindrical heaters and heating jacket.

2.3.8 Load frame, leakoff backpressure regulator, and leakoff collector

The load frame, leakoff backpressure regulator, and leakoff collector are shown in Fig. 2.11. An overburden stress is applied on the conductivity cell by the load frame model CT-250 manufactured by Structural Behavior Engineering Laboratories, Inc. An AP-1,000 pump system used to pressurize hydraulic oil to control the load frame is operated by compressed air. The load frame has a 125-in^2 ram area and is capable of applying 250,000 lbm force. The pressure applied on the core surface is about 10 times the load frame's pressure because the cross-sectional area of the core samples is about 1/10 the load frame's ram area. Hence, applying pressure of 100 psi on the load frame generates about 1,000 psi closure stress on the core samples. The conductivity cell is supported by a rack on the load frame. Thus, only the top piston and the top rock are

moved down when pressure is applied on the load frame.

To prevent the flow between the cell's wall and the rubber around the rocks as described in Section 2.3.1, the differential pressure between the cell pressure and the leakoff pressure should not be over 300 psi. Therefore, we installed a Grove backpressure regulator model SD90W with a pressure range of 10-2000 psi in the leakoff line to control the leakoff pressure. The backpressure regulator is controlled by nitrogen gas. The ratio of the flowline pressure over the nitrogen dome pressure of the backpressure regulator is one. That means the pressure applied to the leakoff line is the same as the outlet pressure from the nitrogen tank. The connection to the pressure gauge is 1/4 in. female NPT thread and the connections to the flow lines and the nitrogen line are 1/8 in. female NPT thread. A gas pressure gauge is installed on the top of the backpressure regulator to monitor the nitrogen dome pressure. A ball valve installed in front of the backpressure regulator is opened while fracturing fluid is pumped and is closed when we perform conductivity measurement. A 25-ml graduated cylinder is used to collect the leakoff fluid on the outlet. Fig. 2.12 is a drawing of the backpressure regulator.

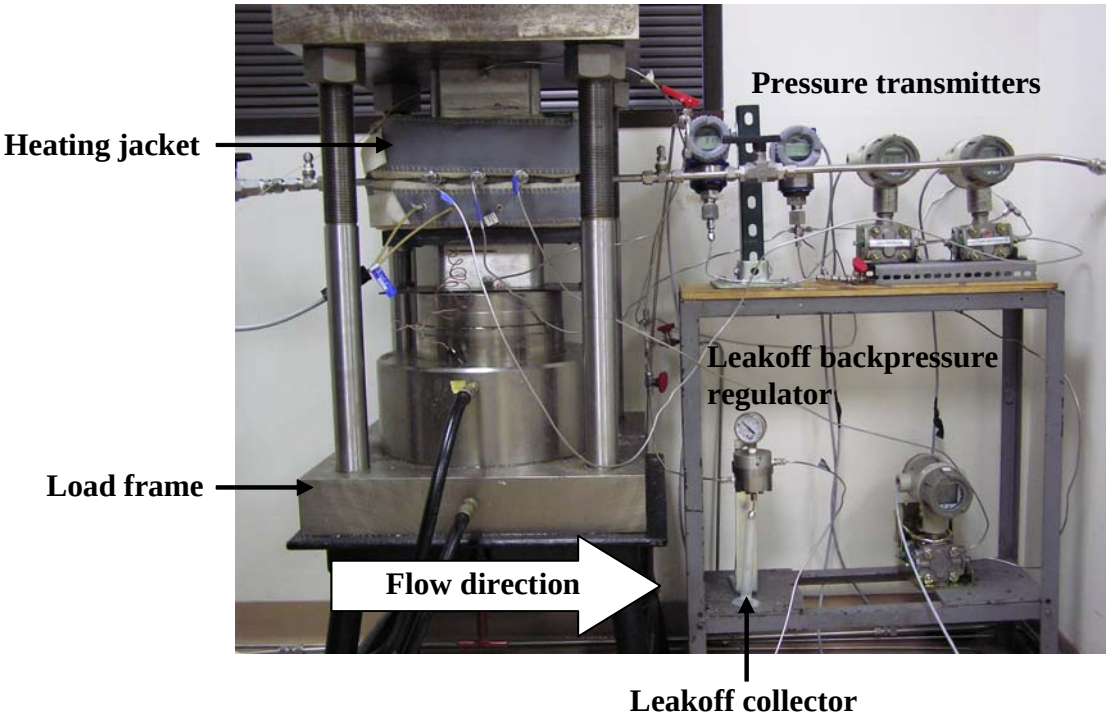

Fig. 2.11- Load frame, pressure transmitters, leakoff backpressure regulator, and leakoff collector.

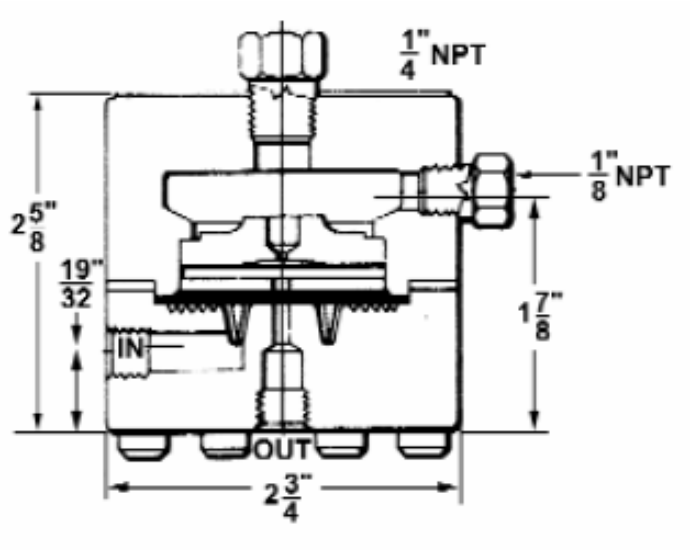

Fig. 2.12- Drawing of the backpressure regulator.

2.3.9 Pressure transmitters and data acquisition system

The experimental data for slurry injection including cell pressure and leakoff pressure and for conductivity measurement including cell pressure and front and back pressure drop along the fracture are digitalized and recorded by using pressure transmitters and data acquisition system. All pressure transmitters are shown in Fig. 2.11. When pumping fracturing fluid, the injection pressure is monitored at the middle port by a FOXBORO gauge pressure transmitter model IGP10-A30E1F-M1 with a calibration range of 0 to 3,000 psi, and the leakoff pressure is detected by a FOXBORO gauge pressure transmitter model IGP10-A22E1F with a calibration range of 0 to 2,000 psi. Two Honeywell pressure transmitters used for conductivity measurement were set up in a previous experiment.[11] One Honeywell differential gauge pressure transmitter was added. The gauge pressure transmitter model STG944R-A10-B07P records the middle point pressure as cell pressure (p_2). Its calibrated range is 0 psi to 125 psi. The differential gauge pressure transmitter model STD 930R-A10-B07P detects the front pressure drop along the fracture (p_1-p_2) and the model STD974-E1A is for the back pressure drop along the fracture (p_2-p_3). Their calibrated ranges are 0 psi to 30 psi and 0 psi to 3,000 psi, respectively. All pressure transmitters have LCD screens to display pressure and are 4 to 20 mA dc analog output. The accuracies of FOXBORO and Honeywell pressure transmitters are 0.05 and 0.075 percent of the upper range value. These pressure transmitters are linked to Acromag Modbus TCP/IP Ethernet I/O modules model 963EN-4012 by 16AWG grade electric cable. The power supplies for both the modbus module and pressure transmitters are 30-watt, 18V, single DC. The pressure transmitters are connected to the filters attached to the pressure access ports and leakoff lines with 1/8-in. stainless steel tubing.

The Acromag modbus TCP/IP module used to transfer the signals to a computer was previously set up for conductivity measurement.[11] It has a direct network interface, processes I/O signals up to 12 channels, and handles power conversion. We added three channels for the two FOXBORO and one Honeywell pressure transmitters. Data

acquisition in the computer is programmed with LabVIEW software form National Instruments. Using LabVIEW 7.0, we modified files, one for slurry injection and one for conductivity measurement, from the previous experiment. Our programs convert the input currents from 4 to 20 mA to pressure values based on the working range of each pressure transmitter. The data is displayed as wave charts in the front panel. At the same time, the pressure readings are exported to Excel spreadsheets named HydSlurryinjectiondata.xls and HydConductivitydata.xls.

2.3.10 High-pressure vessels

Two high-pressure vessels are installed downstream of the conductivity cell to control cell pressure (Fig. 2.13). Currently, no backpressure regulators in the market can handle high concentrations of 30/50 proppant. The proppant particles may plug and/or damage the mechanism inside the backpressure regulator. The high-pressure vessels are modified from core holders with working pressures of 3,000 psi. The inside diameter of the vessels is 5.7 in. and the height is 35 in. A 1/8-in. tube with a needle valve and a 1/2-in. tube with a needle valve are installed in the outlet of each vessel. The flow rates can be adjusted from both valves to achieve high cell pressure. We only use one vessel in each experiment; the other is a backup in case proppant plugs the lines in the other vessel. Flow rate is measured by collecting the fluid from the outlet of the high-pressure vessel.

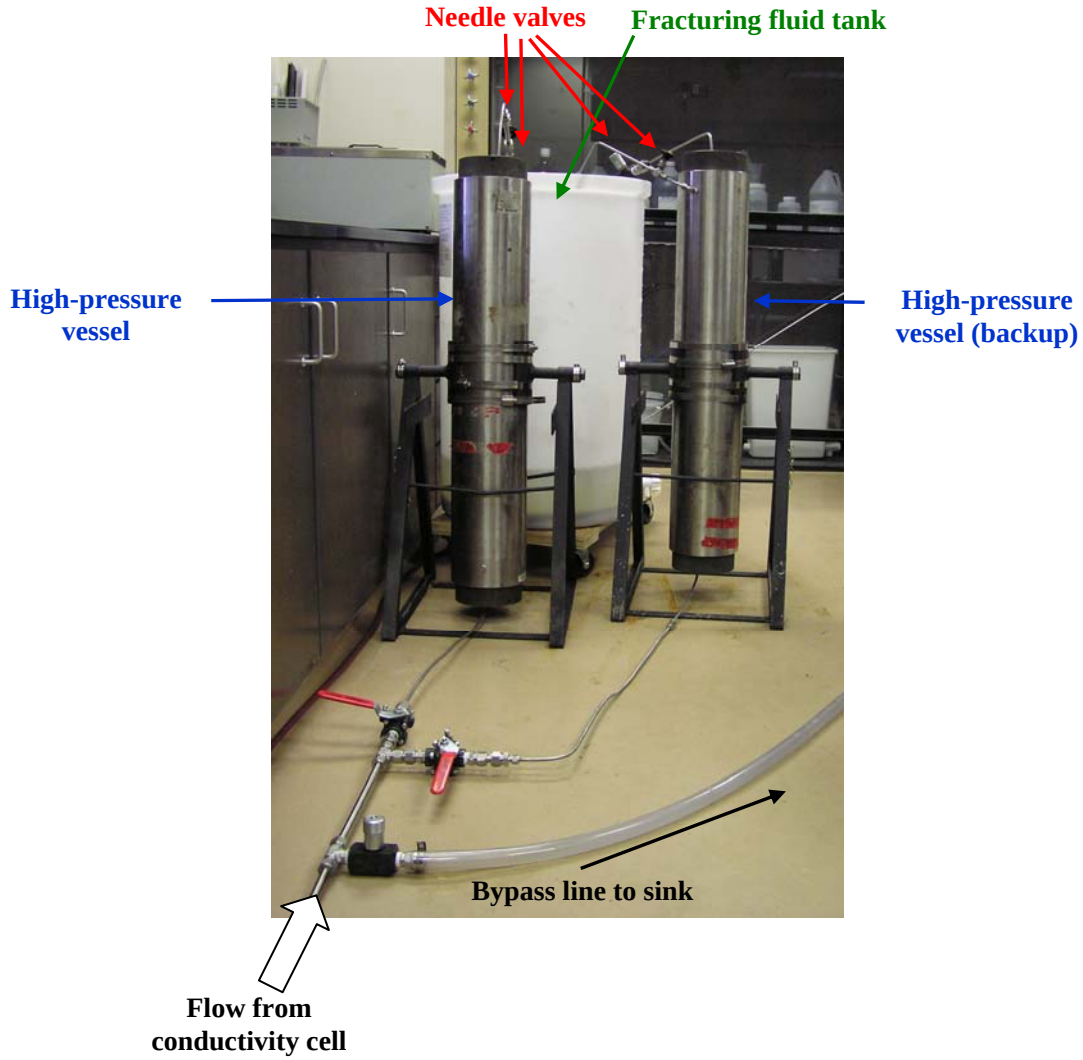

Fig. 2.13- High-pressure vessels.

2.4 Setup of fracture conductivity measurement

The main equipment for conductivity measurement consists of a nitrogen tank to supply gas, a mass flow controller to control and measure gas flow rate, a water chamber to simulate wet gas, a heated conductivity cell under stress of the load frame, and a backpressure regulator to control pressure. Fig. 2.14 shows the schematic of the fracture conductivity laboratory setup. The fracture conductivity is measured by flowing wet

nitrogen gas through the proppant pack, recording pressure drop across the fracture face under five different nitrogen flow rates, and calculating the fracture conductivity by using Forchheimer's equation. The setup is capable of flowing from the leakoff lines to simulate gas flow from the reservoir into the fracture. All flow lines in this experimental setup except the leakoff lines are 1/4-in. stainless steel. The leakoff lines are 1/8-in. stainless steel.

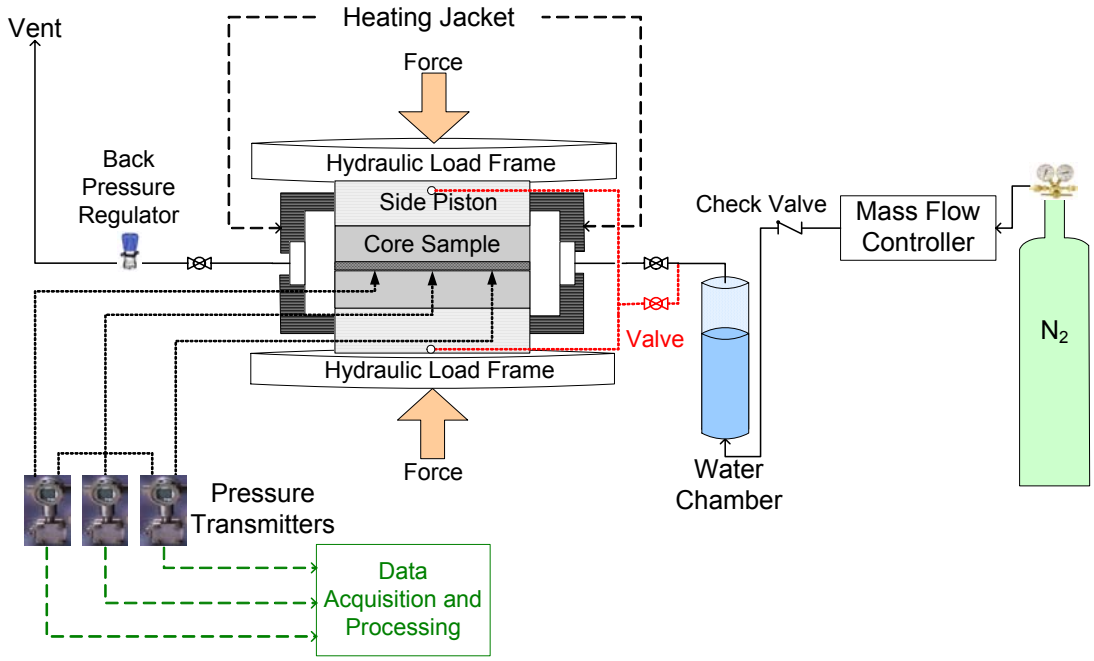

Fig. 2.14- Schematic of dynamic fracture conductivity laboratory setup for conductivity measurement.

The actual experimental setup for fracture conductivity measurement is in Fig. 2.15. Compressed air is used to operate the AP-1,000 pump system that controls the load frame as described in Section 2.3.8. In the first phase of experiments, we have applied 2,000 psi closure stress, which corresponds approximately 200 psi load frame pressure.

Nitrogen flows from a nitrogen tank into an Aalborg nitrogen mass flow

controller model GFC47. The mass flow controller can adjust flow rate from 0 to 100 L/min and the flow rate is shown on a LCD screen. The maximum pressure is 500 psi. To control the mass flow controller, the differential pressure between the outlet of the nitrogen tank and the cell pressure should be over 20 psi. The nitrogen gas flows through a water chamber to generate wet gas. One-way check valves are installed in front of the water chamber's inlet to prevent water from flowing back to the mass flow controller. The gas flows into the heated conductivity cell. An APCO backpressure regulator model 1A with an inlet pressure range of 15 to 300 psi is connected in the outlet from the conductivity cell to achieve constant conductivity cell pressure. In the experiments, the cell pressure is controlled at about 50 psi. The cell pressure and the front and back pressure drop along the fracture are recorded under five different flow rates by pressure transmitters. All the experimental variables are recorded and processed in an Excel spreadsheet to draw the Forchheimer's chart.

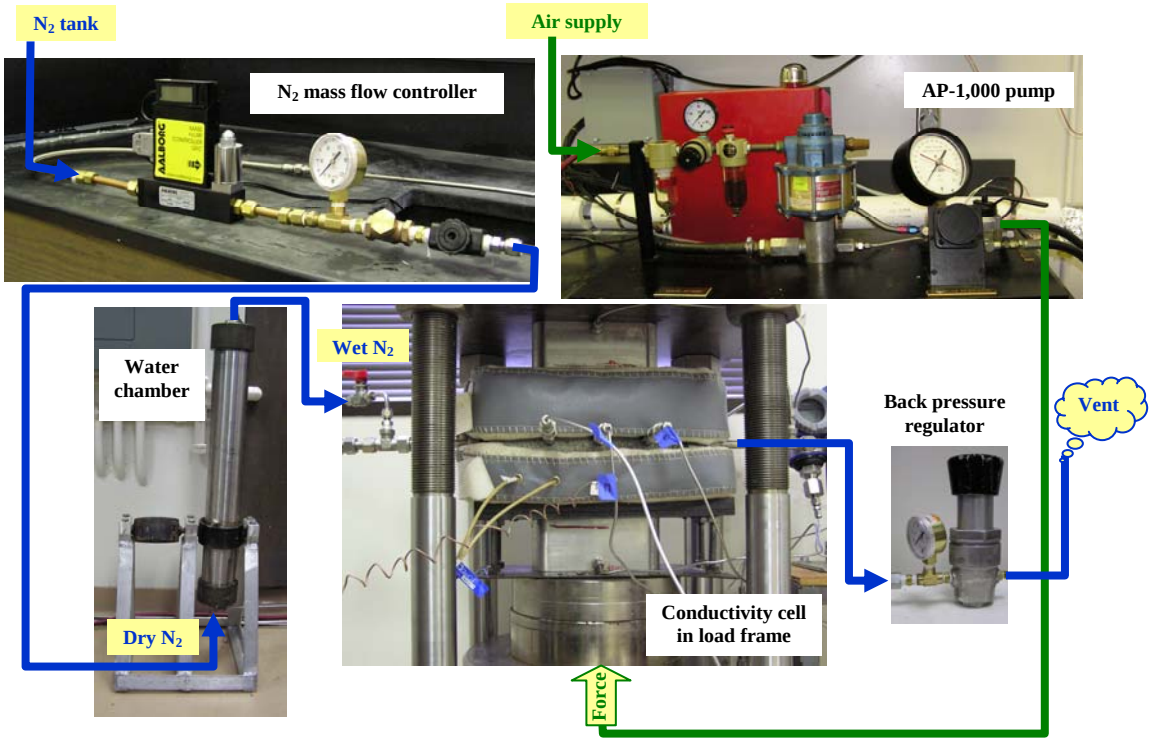

Fig. 2.15- Fracture conductivity measurement experimental setup.

CHAPTER III

EXPERIMENTAL PROCEDURES FOR DYNAMIC FRACTURE CONDUCTIVITY TESTING

3.1 Dynamic fracture conductivity experimental procedure

The experimental procedure consists of five consecutive steps as follows:

- Core sample preparation.
- Rock permeability measurement.
- Fracturing fluid pumping.
- Fracture conductivity measurement.
- Rock permeability and fracture conductivity calculation.

Following is the dynamic fracture conductivity experimental procedure:

1. Prepare the rock samples according to Section 3.2.
2. Assemble the core samples into the conductivity cell (Section 3.3).
3. Put the conductivity cell in the center of the hydraulic load frame.
4. Use a horizontal level meter to make sure that the load frame top plate, the conductivity cell, and the load frame bottom ram are all level.
5. Move the load frame to the neutral position by opening the air supply valve to activate the AP-1,000 hydraulic oil pump. Carefully operate the air pressure regulator and the hydraulic oil pressure regulator to pump hydraulic oil to the load frame. The bottom ram of load frame will move up. Monitor the top piston to just touch the top plate. Remove the shim. The shim thickness is the designed fracture width. Do not apply more pressure to the load frame; otherwise, the fracture will close and the experiment cannot be run. Reset the test gauge to zero.
6. Turn on the laboratory exhaust system.

7. Connect the conductivity cell to the system lines, including the inlet line, the outlet line, two leakoff lines, and three pressure recording lines.
8. Make sure all connections are tightened and all valves are in closed positions. Check also all connections for the leakoff backpressure line from the nitrogen tank (make sure there is sufficient gas) to the backpressure regulator.
9. Connect the dry gas line to the conductivity cell's inlet line.
10. Measure the rock permeability following the measurement guideline in Section 3.5.
11. Open the valves in order to fill tap water into the mixing tank. The water volume is calculated from the pumping time for both pad and slurry injections and the dead volume in the system.
12. Wrap the heating jacket around the conductivity cell.
13. Set the temperature controllers of the cylindrical heaters and the heating jacket to the desired temperature. Turn on the switches to preheat the cylindrical heaters and the heating jacket. Flow water continuously for at least one hour to preheat the cylindrical heaters. The temperature sensor of the cylindrical heaters detects the fluid temperature after heating. Failure to flow water may cause the cylindrical heaters' temperature to increase too high, resulting in tubing burning. The temperature sensor of the heating jacket is attached between the jacket and the conductivity cell, so flowing into the cell not required. Set the temperature controllers 5°F higher and lower than the desired temperature for the upper and lower ranges.
14. Switch the proper valves to flow tap water directly to the high-pressure pumps through the cylindrical heaters, but bypassing the conductivity cell and dumping into a sink.
15. Turn on the high-pressure pumps. Check the connections to confirm no leakage at high pumping pressure.
16. While waiting for the heaters to warm up, mix the fracturing fluid described in Section 3.4.

17. Apply backpressure to the leakoff side by opening the nitrogen regulator to 300 psi less than the desired pumping pressure. After several tests, we concluded that the Teflon tape can prevent leakage if the differential pressure is less than 300 psi. Put a graduated cylinder under the outlet line to collect the leakoff fluid.
18. Open the leakoff valve and prepare the high-pressure vessels' outlet valves.
19. Open the LabVIEW file named "Hyd Slurryinjection.vi" from the laboratory computer linked to the pressure transducers. Calibrate a zero value, then run the program. This file is used to record the pumping pressure and leakoff pressure.
20. Turn on the centrifugal pump used to feed base gel into the high-pressure pump's suction, but with the valve connected to the high-pressure pump remaining closed. The base gel therefore will circulate back into the polyethylene drum.
21. When the fluid temperature reaches the proposed temperature, close the tap water valve and switch the polyethylene drum discharge valves to feed the base gel into the high-pressure pumps. In the meantime, switch the discharge valve at the outlet of the conductivity cell to flow through one of the high-pressure vessels (the other one is a backup in case of plugging) then into the waste drum. For environmental safety, the base gel and slurry require treatment and cannot be dumped directly into the sink.
22. Monitor the cell pressure increases as the fluid fills the high-pressure vessel. When the fluid starts to flow into the waste drum, adjust the discharge valve until the cell pressure rises to the desired pressure.
23. Use a stopwatch and a 2-liter beaker to measure the flow rate after the discharge valve. In the meantime, record the leakoff rate if there is any fluid leakoff.
24. After getting the pumping rate, calculate the crosslinker pumping rate to obtain the desired concentration based on the recipe. Adjust the metering pump to feed the crosslinker at the calculated rate, but do not turn on the metering pump.
25. Flow the base gel continuously for 10 minutes.
26. Switch the proper valves to change from the base gel to slurry pumping. Open the metering pump to inject the crosslinker as the slurry is fed in.

27. Flow the slurry for one minute only. Flowing the slurry too long causes a screen-out effect and results in a wide fracture width after applying closure stress. If the slurry is injected for a very short time, it may not enter into the conductivity cell.
28. Close the inlet and outlet valves of the conductivity cell. Open the bypass valve and continue to flow the slurry. Turn off the metering pump.
29. Fill the mixing tank with water and continue to flow to clean the mixing system. Then, switch to the base gel reservoir and pump all remaining gel.
30. Switch the proper valves to flow tap water directly into the high-pressure pumps and continue to flow for one hour to clean the high-pressure pumps. Failure to clean the pumps properly may cause the proppant to settle down and damage the pumps. During the pump-cleaning process, observe the discharge fluid. If only water comes out, switch the valve to discharge water into the sink.
31. After the high-pressure pumps are cleaned, turn off the pumps. Disconnect the metering pump and clean by pumping water for 10 minutes.
32. Disconnect and clean the high-pressure vessel.
33. Load the chemical wastes into a proper tank for disposal.
34. Record the leakoff volume during pumping. Then, clean the graduated cylinder and prepare to collect fluid after applying closure stress.
35. Apply the closure stress by gradually increasing the air pressure, increasing the closure stress 100 psi every 5 minutes to 2,000 psi closure stress. The gauge pressure of 200 psi means a closure stress of 2,000 psi. In the meantime, slowly release the leakoff backpressure by closing the nitrogen regulator and bleed off the pressure.
36. Leave the heated conductivity cell for 18 hours. Secure the test area to prevent any incidents.
37. After 18 hours, stop the LabVIEW program and save the Excel file in the test result folder. Close the leakoff valve. Record the leakoff volume.
38. Take off the filters for cleaning and reconnect. Failure to clean the filters may result in no pressure reading.

39. Connect the wet gas line to the conductivity cell's inlet line. Nitrogen will flow through the water chamber before entering the conductivity cell.
40. Measure the fracture conductivity, following the designed procedure (Section 3.6).
41. Release the hydraulic load frame pressure. Lower the bottom ram of the load frame.
42. Disconnect all lines from the conductivity cell.
43. Disconnect the conductivity cell assembly by using the hydraulic jack. Disassemble the two pistons first; then carefully push the rock samples out together. Measure the fracture width. Open the samples and observe proppant distribution and gel damage inside the fracture.
44. Clean all components of the conductivity cell.
45. Fill the data in the Excel spreadsheet (Appendix A) created for conductivity calculation using the Forchheimer's equation and analyze the experimental results.

3.2 Core sample preparation

Core samples are custom cut to the conductivity cell with about 0.07 in. less in all dimensions. Each core sample is then put in a mold and potted with silicone potting compound. The silicone rubber around the rocks provides a seal between the core and the conductivity cell. The following is our preparation procedure:

1. Cut the rock sample into half with the rock-cutting machine.
2. Mark the rock samples as XA and XB.
3. Weigh the rock samples.
4. Put duck tapes on the top and bottom surfaces and cut edges with an Exacto knife.
5. Brush the rock with SS4155 01P 3 times, 15 minutes apart.

6. Clean the metal molds and bottom plastic plates with acetone by using cloths. Make sure it is very clean; otherwise, the silicone will not be perfectly attached to the rock sample.
7. Spray Sprayon S00315 on the metal molds and bottom plastic plates 3 times (2 minutes apart). Make sure all surface areas are covered, especially the curves.
8. Assemble the molds, tighten the four bottom and the three side screws, and put the rock samples in the center of the molds.
9. Mix 75 cc of silicone potting compound and 75 cc of silicone curing agent from the RTV 627 022 kit. Stir it thoroughly.
10. Pour the silicone mixture into a syringe barrel. Assemble the injection system.
11. Slowly inject the mixture into the gap between the core sample and the mold until it reaches the top of the rock sample.
12. Remove the duck tapes and put the molds into the oven at 60°C for 15 minutes.
13. Refill the mixture to the top of the rock and put in the oven for 2 to 4 hours.
14. Leave the molds to cool down for at least 3 hours.
15. Carefully remove the samples from the molds.
16. Cut the excess silicone at the edges.
17. Label and weigh the rock samples.

3.3 Conductivity cell assembly procedure

Putting the rock samples into the conductivity cell is the most important part of an experiment. Lack of carefulness when assembling the cell may lead to experimental failure as revealed in Table 3.1.

Table 3.1- Problems caused by careless conductivity cell assembly

Actions	Results
If Teflon tape not carefully wrapped	Fluid flows between the rubber and the mold
If the rocks not carefully put into the cell	The Teflon tape moves and causes flow between the rubber and the mold
If the rocks touch too tightly	The shim cannot be removed
If the shim is not in the center	System cannot record any pressure
If the pistons not touch the rocks	The test result is biased because of the gap in between

We therefore created the following guideline to assemble the conductivity cell:

1. Select core samples for the experiment. Make signs for front, back, top and bottom sides.
2. Trim the silicone rubber in positions that will be attached to the pressure recording lines after applying closure stress to prevent obstructions of the pressure lines.
3. Wrap each core sample with Teflon tape to avoid flow between the rubber and the conductivity cell.
4. Apply Dow Corning high-vacuum grease to the rubber and the Teflon tape.
5. Carefully insert the core samples into the conductivity cell by using the hydraulic jack. Be sure the fracture faces are lined up with the inlet and outlet flow insert ports.
6. Put a 0.25-in. shim slightly above the middle point the cell. When the top piston moves down, the gap will be in the middle point. The shim thickness is the designed fracture width.

7. Apply o-ring grease to the piston o-rings and the flow insert o-rings.
8. Use the hydraulic jack to push the pistons into the cell until they touch the rocks. Make sure the shim is in the middle of the cell at all times.
9. Remove the shim and install the flow inserts.
10. Install the support rack and adjust the bolts to fit the bottom piston.
    The samples are ready to be tested.

3.4 Fracturing fluid mixing procedure

The service company provided the mixing procedure along with all chemicals. The research team adjusted the recipe to the research proposal as in Table 3.2. The general mixing procedure is as follows:

1. Propose pumping volume, temperature, and polymer concentration for an experiment.
2. Measure amount of chemicals required such as HPG polymer in powder form, etc.
3. Add a measured volume of tap water into the mixing tank.
4. Turn on the centrifugal pump and the mixer.
5. Add the HPG gel and pH Buffer #1 to pH 6.5.
6. To ensure hydration, mix the base gel for at least 30 minutes.
7. Measure and record the fluid pH, temperature, and viscosity of the base gel.
8. Transport a volume of pad fluid to the polyethylene drum.
9. Add pH Buffer #2 and pH Buffer #3 to the slurry tank until the target pH is reached.
10. Add gel stabilizer, breaker, and breaker activator.
11. Add proppant to the slurry tank.
12. Mix crosslinker and crosslink accelerator in a bottle and connect to the metering pump.

Table 3.2- Fracturing fluid mixing recipes

Chemical	Temperature (degree F)	
	150	250
Hydroxypropyl guar, lb/Mgal	30	40
pH Buffer #1 to pH	6.5	6.5
pH Buffer #2 to pH	10.0	10.0
pH Buffer #3 to pH	None	11.5
Gel stabilizer, gal/Mgal	0	3.0
Breaker, gal/Mgal	10	5
Breaker activator, gal/Mgal	1.0	0
Borate crosslinker, gal/Mgal	0.9	1.2
Crosslink accelerator, gal/Mgal	0.1	0.1

3.5 Rock permeability measurement

Following is the procedure to measure rock permeability:

1. Adjust the mass flow controller to the closed position. Calibrate to a zero value. Then, connect to the dry gas line.
2. Open the proper valves for gas permeability measurement including the leakoff valve. Do not forget to close the outlet valve (flow nitrogen through the rock samples to the leakoff line).
3. Open the nitrogen regulator to flow gas into the system. Open the mass flow controller.
4. Check the gas flow line to ensure no leakage.
5. Control the gas flow rate by adjusting the mass flow controller.
6. Record the gas flow rate, the cell pressure and the leakoff pressure. Vary the gas flow rates between 1 to 5 L/minute to collect five data sets.
7. Calculate the rock permeability by using the Forchheimer's equation.

8. Disconnect the nitrogen line to prevent liquid from flowing through the line and damaging the mass flow controller.

3.6 Fracture conductivity measurement

Following is a conductivity measurement procedure:

1. Adjust the mass flow controller to the closed position. Calibrate to a zero value. Then, connect to the wet gas line.
2. Open the proper valves to measure fracture conductivity. Remember to close the leakoff valve.
3. Open the nitrogen regulator to flow gas into the system. Open the mass flow controller.
4. Check the gas flow line to ensure no leakage.
5. Open the LabVIEW file named "Hyd Conductivity Pressures.vi" from the laboratory computer linked to the pressure transducers. Calibrate a zero value; then run the program. This file is used to record the cell pressure, the front differential pressure, and the back differential pressure.
6. Adjust the nitrogen regulator, the backpressure regulator and the mass flow controller to get the first point at around 2 L/minutes and 50-psi cell pressure. Keep the differential pressure between the inlet and outlet of the mass flow controller less than 40 psi. After several tests, we found that the differential pressures exceeding 40 psi may cause fluctuating flow rates.
7. Leave the flow rate and the pressures until steady values are observed, normally 5 minutes. Record the gas flow rate, the cell pressure, the front differential pressure and back differential pressure.
8. Vary the gas flow rates between 2 and 10 L/minute to receive five data sets at the constant cell pressure of 50 psi. The cell pressure is controlled by the backpressure regulator.
9. Calculate the fracture conductivity by using Forchheimer's equation.

10. Flow nitrogen at a low rate of 1 L/min for the desired time step such as 1, 3, 6, 12, and 24 hours, then repeat Step 6 to Step 9.
11. Stop the LabVIEW program and save the Excel file in the test result folder.
12. Close the nitrogen regulator and bleed off the pressure. Relieve the conductivity cell pressure.

3.7 Rock permeability calculation

The rock permeability is calculated by using Forchheimer's equation for gas flow.[13]

Forchheimer's liquid equation is defined as:

$$-\frac{dP}{dL} = \frac{\mu v}{k} + \beta \rho v^2 \quad \text{..... (3.1)}$$

When the inertial flow coefficient, β, is small, the Forchheimer's equation is reduced to Darcy's law.

The flux of gas is $\frac{W}{A} = \rho v$. The mass velocity is constant if the cross sectional area is constant. Therefore, we can multiply Eq. 3.1 by ρ:

$$\rho\left(-\frac{dP}{dL}\right) = \rho\left(\frac{\mu v}{k}\right) + \beta(\rho v)^2 \quad \text{..... (3.2)}$$

Substituting the flux, $\frac{W}{A}$ yields:

$$\rho\left(-\frac{dP}{dL}\right) = \frac{\mu W}{kA} + \beta\left(\frac{W}{A}\right)^2 \quad \text{..... (3.3)}$$

Applying the real gas law, $\rho = \frac{pM}{zRT}$,

$$-\frac{M}{zRT}\int_1^2 p\,dp = \left[\frac{\mu W}{kA} + \beta\left(\frac{W}{A}\right)^2\right]\int_1^2 dL \quad \text{..... (3.4)}$$

Integrating and rearranging Eq. 3.4,

$$\frac{p_1^2 - p_2^2}{L} = \frac{2zRT}{M}\left[\frac{\mu W}{kA} + \beta\left(\frac{W}{A}\right)^2\right] \quad \text{..... (3.5)}$$

Replacing $\frac{W}{A}$ with ρv and rearranging Eq. 3.5 yields:

$$\frac{(p_1^2 - p_2^2)M}{2zRTL} = \frac{\mu\rho v}{k} + \beta(\rho v)^2 \quad \text{..... (3.6)}$$

$$\frac{(p_1^2 - p_2^2)M}{2zRT\mu\rho vL} = \beta\frac{\rho v}{\mu} + \frac{1}{k} \quad \text{..... (3.7)}$$

By plotting Eq. 3.7 as a straight line equation, $y = mx + b$, using $\frac{\rho v}{\mu}$ as the x-axis and $\frac{(p_1^2 - p_2^2)M}{2zRT\mu\rho vL}$ as the y-axis, the intercept of the y-axis is the inverse of the permeability and the slope is the inertial flow coefficient, β.

Calculations using Eq. 3.7 are most convenient for units of: p as Pascal, M as kg/mole, T as Kelvin, L as meter, R as J/mol K, μ as Pa.s, ρ as kg/m^3 and v as m/s. In the laboratory, the upstream pressure and the downstream pressure are measured under five different gas flow rates. We calculate the rock permeability by applying other variables in Table 3.3.

Table 3.3- Data used for rock permeability calculation

Cross sectional area *(A)*	12.00	in^2
Length over pressure drop *(L)*	3.00	in.
Compressibility factor *(z)*	1.00	
Universal constant *(R)*	8.3144	J / mol K
Temperature *(T)*	293.15	K
RMM of nitrogen *(M)*	0.028	kg / kg mole
Viscosity of nitrogen *(μ)*	1.759E-05	Pa .s
Density of nitrogen *(ρ)*	1.16085	kg/m^3

3.8 Fracture conductivity calculation

Fracture conductivity is defined as the fracture permeability times the fracture width.

3.8.1 Using Forchheimer's equation

By substituting v with $\frac{q}{wh}$ in Eq. 3.7, Forchheimer's equation for fracture conductivity is:

$$\frac{\left(p_1^2 - p_2^2\right)Mh}{2zRT\mu\rho Lq} = \frac{\beta}{w^2}\frac{\rho q}{\mu h} + \frac{1}{k_f w} \quad \text{..... (3.9)}$$

By plotting Eq. 3.9 as a straight line equation using $\frac{\rho q}{\mu h}$ as the x-axis and $\frac{\left(p_1^2 - p_2^2\right)Mh}{2zRT\mu\rho Lq}$ as the y-axis, the y-intercept is the inverse of the fracture conductivity.

In the experimental studies, we measure the cell pressure and the pressure drop along the fracture under five different gas flow rates. By applying other variables in Table 3.4, we calculate the x and y components and plotted five points, then determine the fracture conductivity by extrapolating the plot to the y-axis. Fig. 3.1 is an example of Forchheimer's plot from the Excel spreadsheet created for dynamic fracture conductivity tests. To study fluid clean up characteristics and gel damage, the fracture conductivity is measured over some length of time until the value stabilizes.

Table 3.4- Data used for fracture conductivity calculation

Width of fracture face *(h)*	1.75	in
Length over pressure drop *(L)*	5.25	in.
Compressibility factor *(z)*	1.00	
Universal constant *(R)*	8.3144	J / mol K
Temperature *(T)*	293.15	K
RMM of nitrogen *(M)*	0.028	kg / kg mole
Viscosity of nitrogen *(μ)*	1.759E-05	Pa .s
Density of nitrogen *(ρ)*	1.16085	kg/m^3

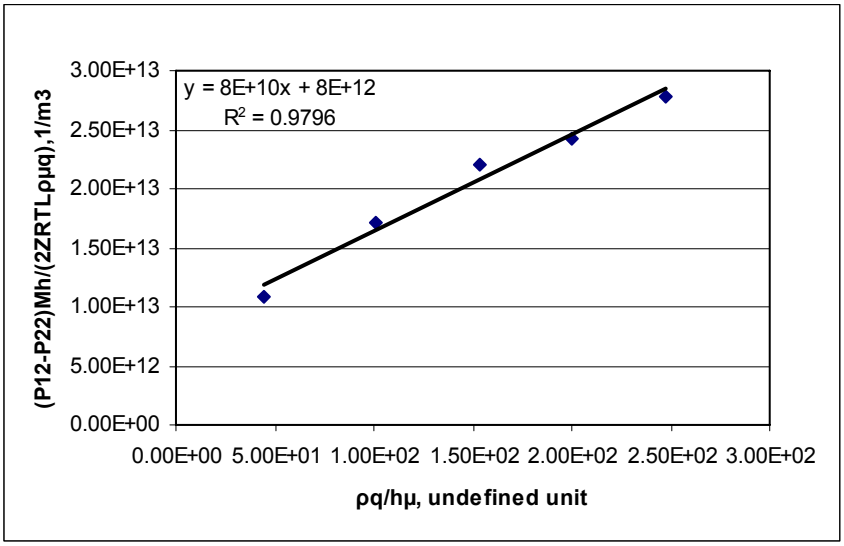

Fig. 3.1- An example of Forchheimer's plot used to calculate fracture conductivity.

3.8.2 Comparing to Darcy's law

From Darcy's law,[14]

$$q(STB/day) = -\frac{1.127\times10^{-3}k(md)A(ft^2)}{\mu(cp)B_g}\frac{dp(psi)}{dL(ft)} \quad \text{..... (3.10)}$$

And $B_g = \frac{V}{V_{sc}} = \frac{znRT/p}{z_{sc}nRT_{sc}/p_{sc}}$ ..... (3.11)

Assuming z and T are constant, $B_g = \frac{p_{sc}}{p}$.

Applying B_g and integrating Eq. 3.10 yields:

$$q(STB/day) = \frac{1.127\times10^{-3}k(md)A(ft^2)\left(\frac{p_1^2 - p_2^2}{2}\right)}{p_{sc}(psi)\mu(cp)L(ft)} \quad \text{..... (3.12)}$$

$$q(STB/day) = \frac{1.127\times10^{-3}k(md)A(ft^2)p_{cell}(psi)\Delta p(psi)}{p_{sc}(psi)\mu(cp)L(ft)} \quad \text{..... (3.13)}$$

Substituting $A = w_{f,after\ closure}h$ yields:

$$q(STB/day) = \left[k(md)w_{f,after\ closure}(ft)\right] \quad \text{..... (3.13)}$$
$$\left[\frac{1.127\times10^{-3}h(ft)p_{cell}(psi)\Delta p(psi)}{p_{sc}(psi)\mu(cp)L(ft)}\right]$$

By plotting Eq. 3.13 as a straight line equation using $\left[\frac{hp_{cell}\Delta p}{p_{sc}\mu L}\right]$ as the x-axis and q as the y-axis, the slope is the fracture conductivity. Fig. 3.2 shows an example of fracture conductivity calculated by using Darcy's law. The slope of 105.04 is the fracture conductivity of 105.04 md-ft.

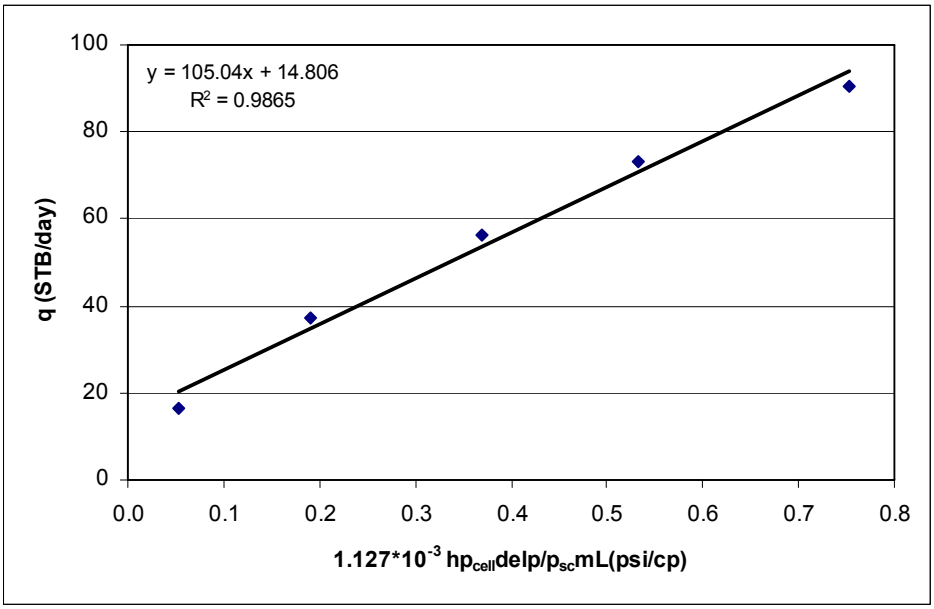

Fig. 3.2- An example of fracture conductivity calculated from Darcy's law.

A comparison of fracture conductivity calculated from Darcy's law and Forchheimer's equation is shown in Fig 3.3. The fracture conductivity calculated from Darcy's law is much lower than calculated by using Forchheimer's equation.

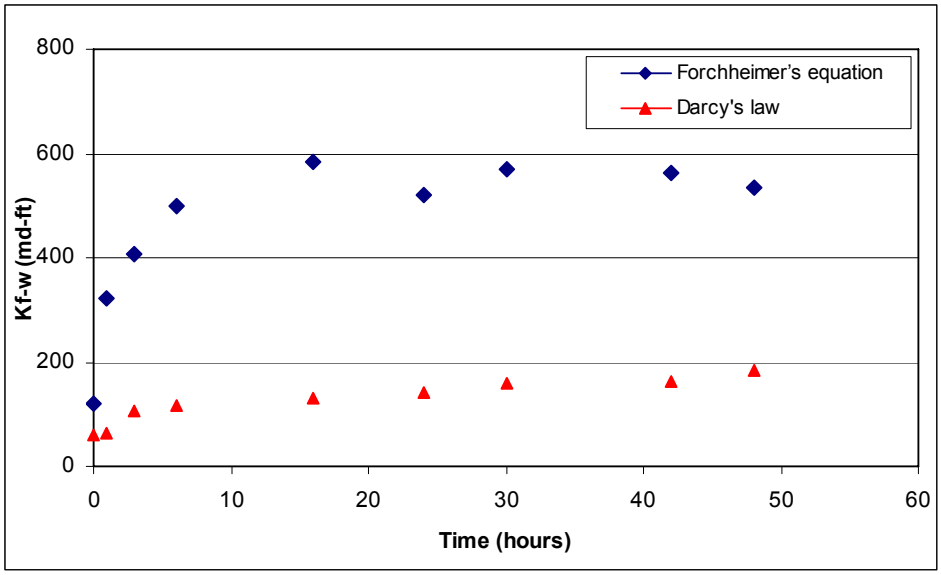

Fig. 3.3- A comparison of fracture conductivity calculated from Darcy's law and Forchheimer's equation.

CHAPTER IV

PRELIMINARY EXPERIMENTS AND RESULTS

After setting up the new laboratory to perform dynamic fracture conductivity tests, we conducted several dry runs to test the operating range of each apparatus. Then, we performed several preliminary experiments for various conditions. Two completed experiments and some lesson learned are described in this chapter.

4.1 Experimental parameters

Table 4.1 presents the parameters in the preliminary tests. The fracturing fluids were mixed following the recipe with the desired polymer concentration and injected into the conductivity cell at the desired temperature. The cell was then shut in for 18 hours to represent the shut-in period. After that, we flowed nitrogen gas through the proppant pack at the desired flow rate to simulate the cleanup period. We repeatedly measured the fracture conductivity at various times until it stabilized.

Table 4.1- Parameters used in the preliminary experiments

Parameters	Experiment A	Experiment B
Desired fracture width, inch	0.25	0.25
Proppant loading, ppg	2	2
Polymer loading, lb/Mgal	30	30
Pumping pressure, psi	320	320
Pumping rate, gal/min	0.75	0.75
Temperature, °F	70	150
Nitrogen flow rate, L/min	1 (dry gas)	1 (wet gas)
Cell pressure during the conductivity measurement, psig	50	50

To ensure the pumping condition in the laboratory is comparable to that of field fracturing jobs, the flux along the fracture in the laboratory is calculated by using Eq.2.3:

$$q_{lab} = v_{lab} w_{f,lab} h_{lab} \quad \text{..... (2.3)}$$

$$v_{lab} = \frac{\left(0.75\ \ gal/\min\right)}{\left(\frac{1.75}{12}\ ft\right)\left(\frac{0.25}{12}\ ft\right)}\left(0.1337\ \ ft^3/gal\right) = 33.0\ \ ft/\min$$

The result in Table 4.2 shows that the flux in the laboratory and the flux calculated from field fracturing jobs are similar.

Table 4.2- Comparison between the field and our laboratory conditions

Parameters	Field	Our Lab
Injection rate	25 bbl/min	0.75 gal/min
Fracture height	100 ft	1.75 in
Fracture width	0.25 in	0.25 in
Flux	33.3 ft/min	33.0 ft/min

4.2 Expected results

To ensure the experimental results were in reasonable ranges, we calculated some variables as references.

4.2.1 Expected surface concentration and fracture width after closure

$$C_s = C_p w_{f,before\ closure} \quad \text{..... (4.1)}$$

$$C_s = \left(2\frac{lb}{gal} \times \frac{7.48\ \ gal}{ft^3}\right)\left(\frac{0.25}{12}\ ft\right) = 0.312\frac{lb}{ft^2} \quad \text{..... (4.2)}$$

$$W_p = C_s A \quad \text{..... (4.3)}$$

$$W_p = \left(0.312 \frac{lb}{ft^2}\right)\left(\frac{12}{144} ft^2\right) = 0.026\ lb \quad \text{..... (4.4)}$$

$$V_p = W_p V_{p,absolute} \quad \text{..... (4.5)}$$

Since the absolute volume of proppant is 0.044 gal/lb,

$$V_p = (0.026\ \text{lb})\left(0.044 \frac{gal}{lb}\right) = 0.00114\ gal \quad \text{..... (4.6)}$$

Assuming proppant porosity of 0.38 yields:

$$V_f = \frac{0.00114\ gal}{(1-0.38)} = 0.00184\ gal \quad \text{..... (4.7)}$$

$$w_{f,after\ closure=} \frac{V_f}{A} = \frac{(0.00184\ gal)\left(\frac{ft^3}{7.48\ gal}\right)}{\left(\frac{12}{144} ft^2\right)} = 0.00295\ ft = 0.0355\ in. \quad \text{..... (4.8)}$$

Therefore, the expected surface concentration is 0.312 lb/ft^2 and the expected fracture width after closure is 0.0355 in.

4.2.2 Expected fracture permeability

The permeability at 250°F under 2,000 psi closure stress of 30/50 Econoprop is reported by CARBO Ceramics to be 230 Darcies.[15] This permeability is used as an upper limit because the proppant permeability was tested with no gel damage. Additionally, the expected permeability was calculated by using Kozeny-Carman's equation.[16]

$$k_f = \frac{\phi^3}{CS_0^2(1-\phi)^2} \quad \text{..... (4.9)}$$

where $S_0 = \frac{6}{d}$, and C is the Kozeny-Carman constant.

Since the median particle diameter is 0.020 in. or 512 micron, C equals 5 for flow through unconsolidated porous media, and the assumed proppant porosity is 0.38, the expected permeability using the Kozeny-Carman equation is:

$$k_f = \left[\frac{(0.38)^3}{5\left(\frac{6}{512\times10^{-6}}\right)^2 (1-0.38)^2} m^2 \right] \left(\frac{Darcies}{9.869\times10^{-13} m^2} \right) = 210.65 \ Darcies \quad . \text{ (4.10)}$$

Both reference permeabilities indicate that the expected permeability should be about 200 Darcies.

4.2.3 Expected fracture conductivity

From the reference permeability of 230 Darcies and the expected fracture width after closure of 0.0355 in., the expected fracture conductivity should be a maximum of 680 md-ft.

4.2.4 Expected pressure drop along the fracture

From Eq.3.13,

$$q(STB/day) = \frac{1.127\times10^{-3} k(md) A(ft^2) p_{cell}(psi) \Delta p(psi)}{p_{sc}(psi)\mu(cp)L(ft)} \quad \text{..... (3.13)}$$

$$A = w_{f,after\ closure} w_{fracture\ face} = \left(\frac{0.0355}{12}\right)\left(\frac{1.75}{12} ft^2\right) = 4.314\times10^{-4} ft^2$$

Using the reference permeability from CARBO ceramics of 230 Darcies and nitrogen viscosity of 0.0176 cp yields:

$$1\ L/\min \times \left(\frac{9.057 STB/day}{L/\min} \right)$$
$$= \frac{1.127 \times 10^{-3} (230{,}000\ Darcies)(4.314 \times 10^{-4}\ ft^2)(64.7\ psi)\Delta p(psi)}{(14.7\ psi)(0.0176 cp)\left(\frac{5.25}{12}\ ft \right)}$$

Thus, $\Delta p = 0.14\ \ psi$.

Since the reference permeability of 230 Darcies is the upper limit, the pressure drop along the fracture at the nitrogen flow rate of 1 L/min should be more than 0.14 psi.

4.3 Preliminary experimental results

4.3.1 Experiment A

Experiment A was conducted at room temperature and the water chamber was not used to wet the nitrogen before it entered the cell. Figs. 4.1 and 4.2 revealed that the experimental conductivity and permeability are higher than expected. The picture of the core samples (Fig. 4.3) shows that the proppant was not uniformly placed in the fracture. The surface concentration is just about 0.2 lb/ft^2. We believe that this was caused by the inlet and outlet valves of the conductivity cell were leak during pump cleaning. Therefore, the line system was modified to prevent water from flowing into the conductivity cell during the pump cleaning.

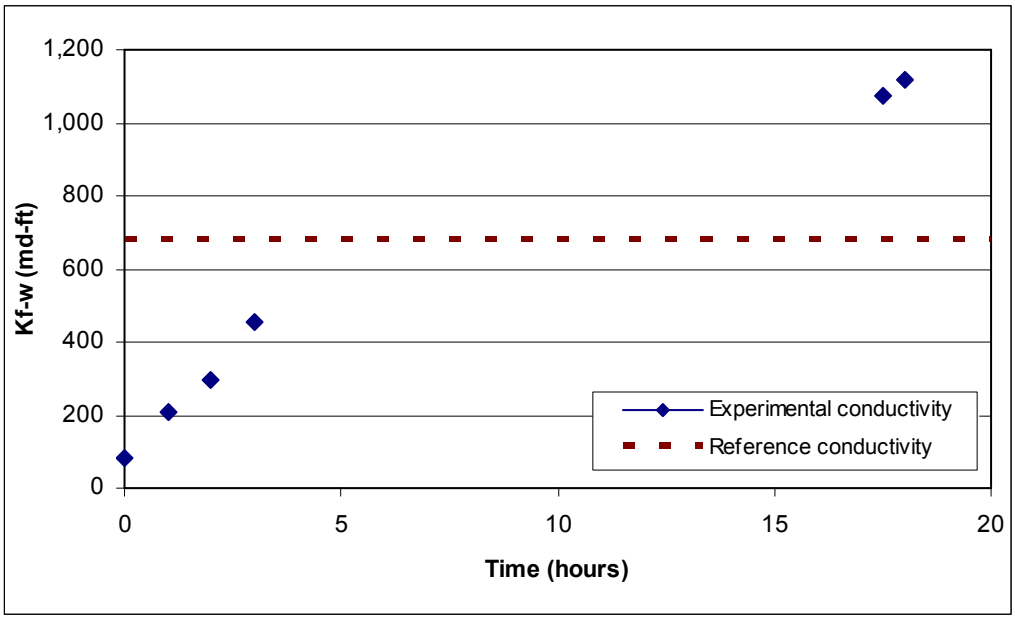

Fig. 4.1- Fracture conductivity over time of Experiment A.

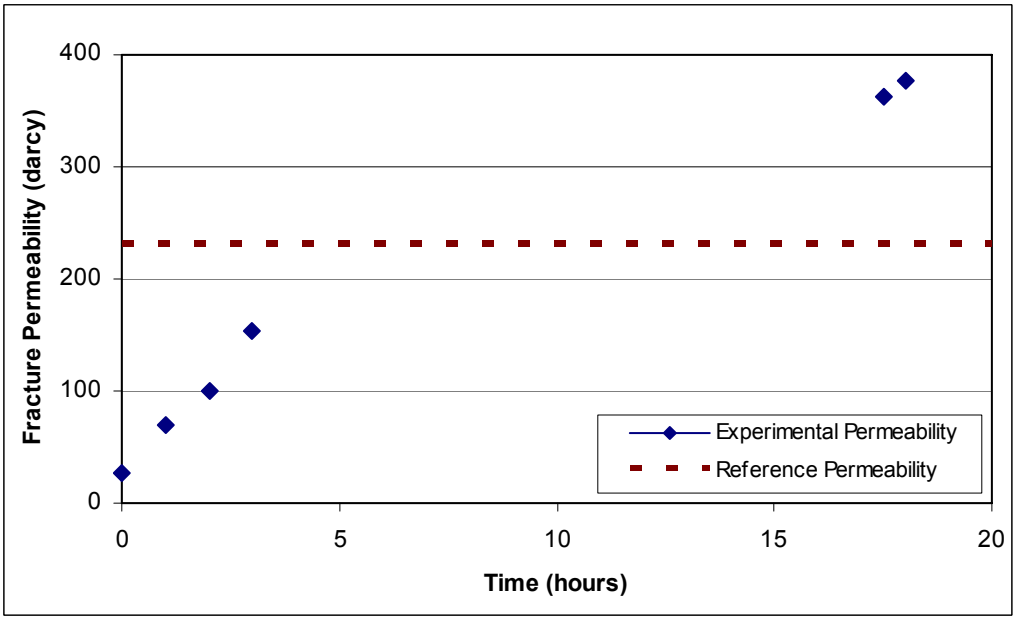

Fig. 4.2- Fracture permeability over time of Experiment A.

Fig. 4.3- Proppant placement of Experiment A.

4.3.2 Experiment B

After modifying the flow system, we successfully conducted Experiment B at a temperature of 150°F with nitrogen flowing through the water chamber. Figs. 4.4 and 4.5 show that the experimental conductivity and permeability are in reasonable ranges. The picture of the core samples (Fig. 4.6) indicated that the proppant was uniformly placed. The surface concentration of 0.39 lb/ft^2 is comparable to the expected surface concentration of 0.31 lb/ft^2.

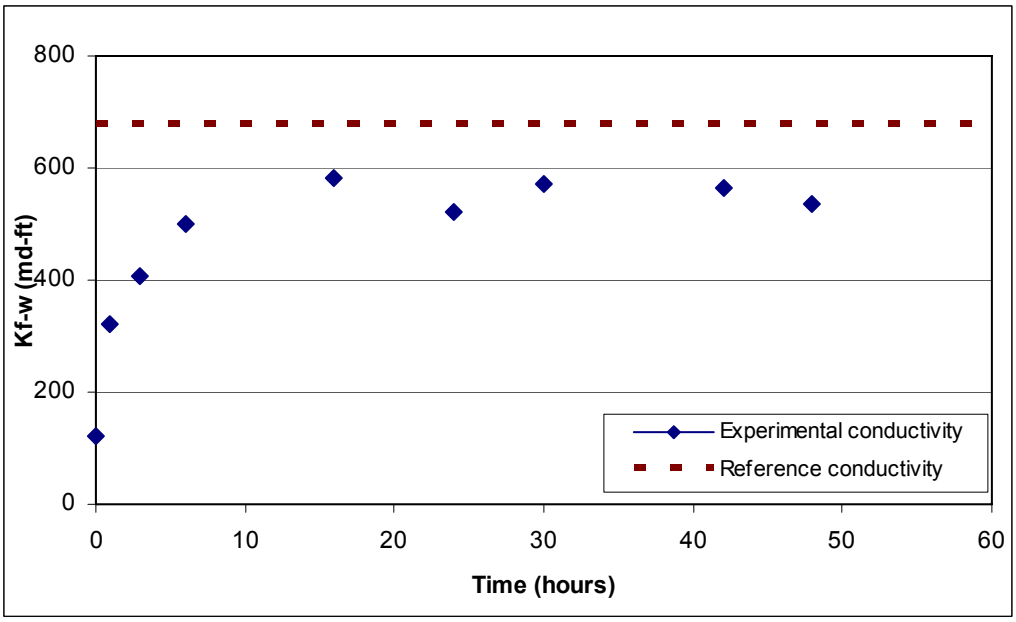

Fig. 4.4- Fracture conductivity over time of Experiment B.

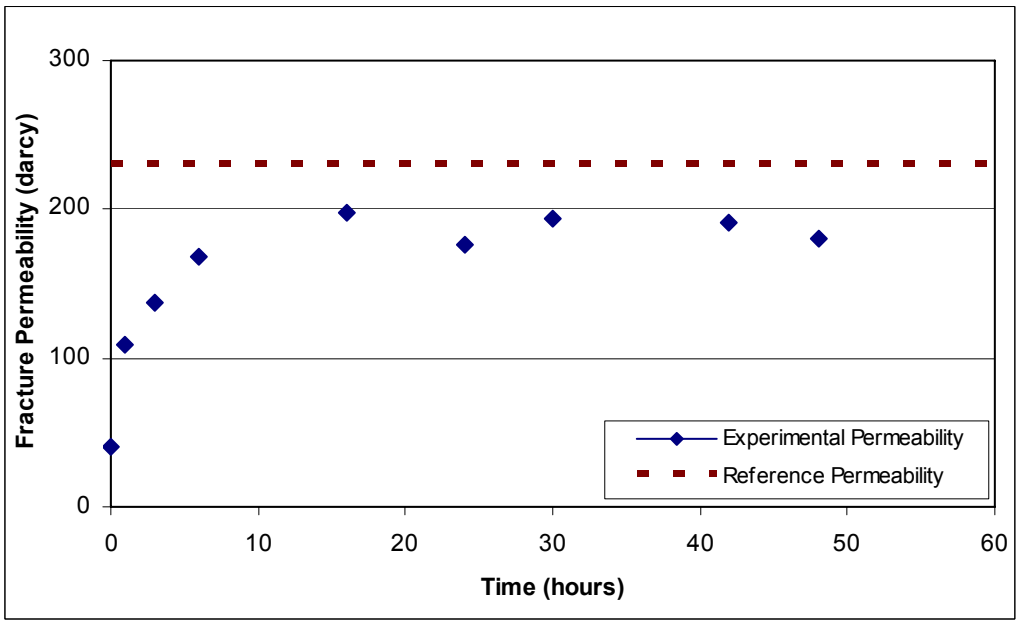

Fig. 4.5- Fracture permeability over time of Experiment B.

Fig. 4.6- Proppant placement of Experiment B.

4.4 Lesson learned

Lesson learned during the experimental setup are described below.

4.4.1 Mixing system

The original design was to use a magnetic stirrer and a stirrer bar to mix slurry as illustrated in Fig. 4.7. We found that the proppant in the bottom around the stirrer bar could not move; therefore, the mixture was not uniformly mixed.

Fig. 4.7- A magnetic stirrer and a created vortex.

The next design was to mix a base gel in the tank by using a centrifugal pump to circulate fluid. Then, we fed proppant on the fly from a container into the flowline by rotating a ship auger bit (Fig. 4.8). However, this design was unsuccessful because fluid flows into the proppant container.

Fig. 4.8- A ship auger bit.

4.4.2 Plunger pump

Initially, we designed to use a Bran & Lubbe simplex plunger pump (Fig. 4.9) which was available from the Harold Vance Department of Petroleum Engineering at Texas A&M University and fit to the application conditions. These pumps had been used by an oil company in similar experiments. After 2-month trials with some guidance from the company's representative, we concluded that these pumps with spring valves cannot pump slurry at high pressure because proppant particles prevent the valves from fully closing (Fig. 4.10).

Fig. 4.9- Bran & Lubbe simplex plunger pump.

Fig. 4.10- Proppant particles prevent the valves from fully closing.

4.4.3 Screen out

The slurry was injected for five minutes in the first preliminary experiment to ensure that the proppant was placed in the conductivity cell. After opening the cell, however, we found that the fracture width after closure was much higher than the expected value (Fig. 4.11). After investigating, we concluded that the pumping time was too long. The flow leaving choked at the outlet of the conductivity cell led to the screen

out. After several experiments, we concluded that slurry pumping of one minute is an optimal point; with no screen out and proppant placed uniformly in the conductivity cell.

Fig. 4.11- A screen out experiment.

4.4.4 Gas bypassing

During the first experiment, the pressure drop along the fracture is almost zero. This was caused by gas flowing in the gap between the cores and the cell body (Fig. 4.12). To avoid experimental failure, the silicone rubber must fully cover the core samples.

Fig. 4.12- Gas bypassing.

4.4.5 Sealant between the silicon rubber and the wall of conductivity cell

Before using the Teflon tape to prevent the flow between the silicon rubber and the wall of conductivity cell, several varieties of epoxy (Fig. 4.13) were tried with no success.

Fig. 4.13- Varieties of epoxy.

4.4.6 Backpressure regulator

Originally, we designed to install a Tescom backpressure regulator Model 54-2165-24A (Fig. 4.14) in the flowline after the conductivity cell to achieve high pressure of 1,000 psi. After testing, the backpressure regulator went out of service. In the meantime, we found that the particles stuck in 1/8-in. tubing. We believe that the particles also stuck in the 1/8-in. profile inside the backpressure regulator. We decided not to use the backpressure regulator even though the company claimed that its regulator would work in our conditions.

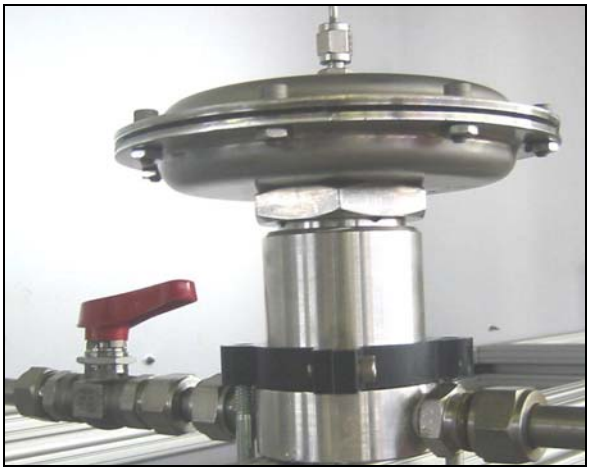

Fig. 4.14- Tescom backpressure regulator.

CHAPTER V

CONCLUSIONS AND RECOMMENDATIONS

5.1 Conclusions

The objectives of this project were to design and set up an experimental apparatus for dynamic fracture conductivity testing and create a fracture conductivity test workflow standard. This new approach will be used in future studies of fracturing fluid cleanup characteristics and gel damage.

We carefully designed the hydraulic fracturing laboratory to provide appropriate scaling of the field conditions experimentally. The specifications for each apparatus were carefully considered with flexibility for further studies and the capability of each apparatus was defined. We created the workflow standard to be a guideline for future experiments. Some dry runs and preliminary experiments performed with sandstone showed that following the procedure allows the experiment to run smoothly.

We reached some conclusions from the preliminary experimental results:

- By using proper equipment and following the procedure, the fracturing treatment in the fields can be simulated at the laboratory scale.
- The proppant is placed uniformly even under dynamic conditions.
- Reservoir fluid helps clean up the residues and results in higher fracture conductivity.

5.2 Recommendations for future hydraulic fracture research work

For future studies in fracturing fluid cleanup characteristics and gel damage investigation, parameters such as polymer concentration, proppant type, proppant loading, injection rate and time, fluid and cell temperature, desired fracture width, and gas flow rate after shut-in should be considered. Factors such as fracture conductivity

changing with time, proppant pack pattern, amount of proppant in the fracture, and gel damage should be investigated in detail. Some studies on yield stress should be performed. Experiments following the API RP 61 should be conducted to define reference points for comparison.

NOMENCLATURE

A	=	Cross-sectional area (in^2)
B_g	=	Gas formation volume factor (res cf/SCF)
C	=	Kozeny-Carman constant
C_p	=	Proppant concentration (ppg)
C_s	=	Surface concentration (lb/ft^2)
D	=	Diameter (in.)
h	=	Fracture height (ft)
L	=	Length over pressure drop (in.)
M	=	Molecular mass (kg/kg mole)
p_1	=	Upstream pressure (psi)
p_2	=	Downstream pressure (psi)
q	=	Fluid flow rate (L/min)
R	=	Universal gas constant (J/mol K)
T	=	Temperature (K)
v	=	Fluid flux (ft/min)
V_f	=	Fracture volume (gal)
V_p	=	Proppant volume (gal)
W	=	Mass flow rate (kg/min)
w_f	=	Fracture width (ft)
W_p	=	Proppant weight (lb)
x_f	=	Fracture length (ft)
z	=	Compressibility factor of gas (Dimensionless)
ρ	=	Density (lbm/ft^3)
μ	=	Fluid viscosity (cp)
β	=	Inertial flow coefficient (1/ft)

REFERENCES

1. Gidley, J.L., Holditch, S.T., Nierode, D.E., and Veatch, R.W. Jr.: *Recent Advances in Hydraulic Fracturing*, Monograph Series, SPE, Richardson, Texas (1989) **12**, 1.
2. Gidley, J.L., Holditch, S.T., Nierode, D.E., and Veatch, R.W. Jr.: *Recent Advances in Hydraulic Fracturing*, Monograph Series, SPE, Richardson, Texas (1989) **12**, 135.
3. *RP 61, Recommended Practices for Evaluating Short Term Proppant Pack Conductivity*, first edition, API, Washington, DC (1989).
4. Cooke, C.E. Jr.: "Effect of Fracturing Fluids on Fracture Conductivity," *JPT* (October 1975) 1273-1282.
5. Almond, S.W. and Bland, W.E.: "The Effect of Break Mechanism on Gelling Agent Residue and Flow Impairment in 20/40 Mesh Sand," paper SPE 12485 presented at the 1984 SPE Formation Damage Control Symposium, Bakersfield, California, 13-14 February.
6. Roodhart, L.P., Kulper, T.O.H., and Davies, D.R.: "Proppant-Pack and Formation Impairment During Gas-Well Hydraulic Fracturing," paper SPE 15629 presented at the 1986 SPE Annual Technical Conference and Exhibition, New Orleans, 5-8 October.
7. Penny, G.S.: "An Evaluation of the Effects of Environmental Conditions and Fracturing Fluids Upon the Long-Term Conductivity of Proppants," paper SPE 16900 presented at the 1987 SPE Annual Technical Conference and Exhibition, Dallas, 27-30 September.
8. Parker, M.A. and McDaniel, B.W.: "Fracturing Treatment Design Improved by Conductivity Measurements Under In-Situ Conditions," paper SPE 16901 presented at the 1987 SPE Annual Technical Conference and Exhibition, Dallas, 27-30 September.

9. Hawkins, G.W.: "Laboratory Study of Proppant-Pack Permeability Reduction Caused by Fracturing Fluids Concentrated During Closure," paper SPE 18261 presented at the 1988 SPE Annual Technical Conference and Exhibition, Houston, 2-5 October.
10. McDaniel, B.W.: "Use of Wet Gas Flow for Long-Term Fracture Conductivity Measurements in the Presence of Gel Filter Cakes," paper SPE 17543 presented at the 1988 SPE Rocky Mountain Regional Meeting, Casper, Wyoming, 11-13 May.
11. Zou, C.: "Development and Testing of an Advanced Acid Fracture Conductivity Apparatus," MS thesis, Texas A&M U., College Station, Texas (2006).
12. Carslaw, H.S. and Jaeger, J.C.: *Conduction of Heat in Solids*, Oxford University Press, Oxford, the United Kingdom (1986) 62-64.
13. Pursell, D. A.: "Laboratory Investigation of Inertial Flow in High Strength Fracture Proppants," MS thesis, Texas A&M U., College Station, Texas (1987).
14. Economides, M.J., Hill, A. D., and Ehlig-Economides, C.: *Petroleum Production Systems*, Prentice Hall PTR, Upper Saddle River, New Jersey (1993).
15. "Long Term Conductivity," CARBO Ceramics, www.carboceramics.com/English/products/ec_2.html, 15 June 2007.
16. Jin, G., Patzek, T.W., and Silin, D.B.: "Direct Prediction of the Absolute Permeability of Unconsolidated and Consolidated Reservoir Rock," paper SPE 90084 presented at the 2004 SPE Annual Technical Conference and Exhibition, Houston, 26-29 September.

APPENDIX A

Hydraulic Fracture Testing Data Sheet

Test Number: _____ Start Time: _____ Date: _____

Rock Number: _____ End Time: _____ Labview data ☐

1 *Test Parameters:*

Desired fracture width	_____ inch	Pumping pressure	_____ psi
Gas flowrate	_____ L/min	Leakoff backpressure	_____ psi
Proppant loading	_____ ppg	Temperature	_____ F
Polymer loading	_____ lb/Mgal		

2 *Rock Permeability Measurement:*

Gas flowrate (L/min)	Δ P Leakoff (psi)
_____	_____
_____	_____
_____	_____
_____	_____

3 *Fracture Fluid Mixing:*

Polymer Mixing		Slurry Mixing	
Water volume	_____ gallons	Water volume in the tank	_____ gallons
Polymer	_____ grams	Proppant weight	_____ grams
pH buffer#1	_____ ml		
pH buffer#2	_____ ml	Crosslinker	
pH buffer#3	_____ ml	Crosslinker	_____ ml
Gel stabilizer	_____ ml	Crosslinker accelerator	_____ ml
Breaker	_____ ml	Injected rate	_____ ml/min
Breaker activator	_____ ml		

4 *Pumping:*

Pumping rate	_____ L/min	Temperature reading	_____ F
Pad pumping time	_____ minutes	Cell pressure reading	_____ psi
Slurry pumping time	_____ minute	Leakoff backpressure	_____ psi
		Δ P Fracture	_____ psi

5 *Leakoff Measurement:*

Time (min)	Leakoff volume (ml)
_____	_____
_____	_____
_____	_____
_____	_____

6 *Conductivity Testing:*

Start Shut-in Time:	_____
Load from Frame:	_____ psi
Start Flow N2 Time:	_____
End Flow N2 Time:	_____
N2 tank inflow pressure	_____ psi
Gas flowrate	_____ L/min

7 *After Conductivity Testing:*

Weight of proppant	_____ grams
Width of proppant	_____ inch

Fig. A.1- Hydraulic fracturing experiment data sheet.

Conductivity Data Sheet

Test Number: _____ N_2 flow rate (L/min) _____ Labview data ☐ L/min Date: _____

Time (hrs)	Overburden Load		Point	Time	N_2 Pressure		Flowrate	Cell Pressure		
	Load from Frame	P_{air}			after tank	after flow meter		P_{Cell}	ΔP Front	ΔP Back
	psi	psi			psi	psi	LPM	psi	psi	psi
						Calibration point				
0			1							
			2							
			3							
			4							
			5							
			6							
			7							
1			1							
			2							
			3							
			4							
			5							
			6							
			7							
3			1							
			2							
			3							
			4							
			5							
			6							
			7							
6			1							
			2							
			3							
			4							
			5							
			6							
			7							
16			1							
			2							
			3							
			4							
			5							
			6							
			7							
24			1							
			2							
			3							
			4							
			5							
			6							
			7							
30			1							
			2							
			3							
			4							
			5							
			6							
			7							

Fig. A.2- Fracture conductivity experiment data sheet.

Experiment Date	21-Apr-07
Test Number	6
Rock Number	1A&1B
Fracturing Conditions	
Polymer loading, lbm	30
Pumping rate, gal/min	0.75
Pressure, psi	320
Temperature, F	150

Data used for calculations

Length of fracture over pressure drop (in) =	5.25
Width of fracture face (in) =	1.75
RMM of nitrogen (kg / mole) =	0.028
Compressibility factor, Z =	1.00
R (J / mol K) =	8.3144
Temperature, T (K) =	293.15
Viscosity of nitrogen (Pa .s) =	1.75923E-05
Density of nitrogen (kg/m^3) =	1.16085
Standard pressure (psi) =	14.7
Overburden ram area (in^2) =	125
Rock surface area (in^2) =	12.00

In the fracture

Fracturing width before closeure (in) =	0.25
Proppant concentration (ppg) =	2
Assume porosity =	0.38
Proppant surface concentration (lb/ft2) =	0.312
Weight of proppant in fracture (lb) =	0.026
Volume of proppant (gal)	0.00114
Volume of fracture (gal)	0.00184
Fracturing width after closeure (in) =	0.03415

Calculations

Time (hrs)	Overburdern Pressure (psi)	Flowrate (LPM)	P_1 (psi)	P_2 (psi)	$P_1^2 - P_2^2$ (atm^2)	y-axis, $(P_1^2-P_2^2)Mh/(2ZRTL\rho\mu_{q),1/m^3}$	x-axis, rq/hμ, undefined unit	Intercept from Graph	k_f-w (md-ft)	Permeability,darcy
0	2083	4.6	72.02	67.59	2.86	3.60E+13	1.14E+02	2.76E+13	**120.38**	**42.31**
		6.6	69.37	60.55	5.30	4.64E+13	1.63E+02			
		8.0	70.21	59.78	6.27	4.53E+13	1.98E+02			
		10.0	72.91	58.89	8.55	4.94E+13	2.47E+02			
1	2083	2.1	68.68	67.93	0.47	1.31E+13	5.20E+01	1.04E+13	**320.56**	**112.65**
		3.6	68.72	65.90	1.76	2.82E+13	8.91E+01			
		6.0	71.26	65.00	3.95	3.80E+13	1.48E+02			
		8.2	70.97	60.96	6.11	4.31E+13	2.03E+02			
		9.8	71.25	58.64	7.58	4.47E+13	2.42E+02			
3	2083	1.8	68.88	68.35	0.34	1.08E+13	4.45E+01	8.16E+12	**407.21**	**143.10**
		4.1	67.90	65.94	1.21	1.71E+13	1.01E+02			
		6.2	68.42	64.59	2.36	2.20E+13	1.53E+02			
		8.1	68.44	62.85	3.40	2.42E+13	2.00E+02			
		10.0	71.31	63.62	4.80	2.78E+13	2.47E+02			
6	2083	2.6	65.33	64.58	0.45	1.00E+13	6.43E+01	6.67E+12	**498.65**	**175.24**
		4.9	68.96	66.86	1.32	1.56E+13	1.21E+02			
		6.4	69.67	66.53	1.98	1.79E+13	1.58E+02			
		8.1	70.65	66.17	2.84	2.02E+13	2.00E+02			
		10.7	71.19	64.17	4.40	2.38E+13	2.65E+02			
16	2083	1.6	66.82	66.47	0.22	7.80E+12	3.96E+01	5.70E+12	**583.19**	**204.95**
		4.7	67.54	65.58	1.21	1.49E+13	1.16E+02			
		6.6	67.31	65.03	1.40	1.22E+13	1.63E+02			
		8.4	67.10	62.23	2.91	2.01E+13	2.08E+02			
		10.4	68.34	62.04	3.80	2.11E+13	2.57E+02			

Fig. A.3- Fracture conductivity calculation spreadsheet.

VITA

Name:	Potcharaporn Pongthunya
Address:	46 Sriwangtan Road Banpong Ratchaburi 70110 Thailand
Email Address:	yok_pe@yahoo.com
Education:	B.Eng., Petroleum Engineering, Chulalongkorn University, 2002 Bangkok, Thailand
	M.S., Petroleum Engineering, Texas A&M University, 2007 College Station, Texas, U.S.A.
Employment History:	Chevron Offshore (Thailand) Ltd., 2002 - 2005

This thesis was typed by the author.